Received: 15 April 2020 | Revised: 22 March 2021 | Accepted: 24 March 2021

DOI: 10.1002/esp.5125

RESEARCH ARTICLE

ESPL WILEY

Mega-scale glacial lineations formed by ice shelf grounding in the Canadian Beaufort Sea during multiple glaciations

Michael Riedel[1] | Scott Dallimore[2] | Michael Wamsteeker[3] | Gary Taylor[4] | Edward L. King[5] | Kristin M. M. Rohr[2] | Jong Kuk Hong[6] | Young Keun Jin[6]

[1]GEOMAR Helmholtz-Centre for Ocean Research Kiel, Kiel, Germany

[2]Natural Resources Canada, Geological Survey of Canada, Sidney, British Columbia, Canada

[3]ExxonMobil, Calgary, Alberta, Canada

[4]Formerly Imperial Oil Resources, Calgary, Alberta, Canada

[5]Natural Resources Canada, Geological Survey of Canada, Dartmouth, Nova Scotia, Canada

[6]Korea Polar Research Institute (KOPRI), Incheon, South Korea

Correspondence
Michael Riedel, GEOMAR Helmholtz-Centre for Ocean Research Kiel, Wischhofstr. 1-3, 24148 Kiel, Germany.
Email: mriedel@geomar.de

Funding information
Ministry of Oceans and Fisheries, Korea, Grant/Award Number: 20160247; Geological Survey of Canada-Pacific; British Petroleum Canada; Imperial Oil Resources Canada Ltd

Abstract

Mega-scale glacial lineations formed by the raking of ice shelves across the seafloor have been reported from multiple polar regions. Here, we present the first evidence of continental slope situated buried lineations in the southern Canadian Beaufort Sea in present-day water depths of 220 to 800 m. Three separate surfaces with lineations are defined at sub-seafloor depths of 40 m to 390 m. All lineations are mostly parallel to the general trend of slope contours. The uppermost surface is recognized over a distance of 56 km. In water depths > 500 m the lineations are parallel to each other at a consistent direction (43°–44°). The second lineated surface is a regionally occurring erosional unconformity. This event has two sub-sets of lineations: mid-slope situated lineations oriented at 42°–48°, and lineations closer to the continental shelf break at 55°–59°. The third lineated surface is an unconformable horizon buried up to 390 m below seafloor with lineaments oriented between 30° and 55°. All three sets of lineations are interpreted to have been produced by ice-ploughing on the paleo-seafloor through the grounding of an ice shelf. Our observations are similar to those documented along the slope off northern Alaska, Chukchi Rise, and Lomonosov Ridge. Collectively, these observations support the concept of an extensive ice shelf across the Arctic Ocean that grounded locally along its margins during multiple glaciations, including during the penultimate (or an earlier) glaciation. The youngest set of lineations indicates ice movement to the southwest with a suggested source in Amundsen Gulf and/or M'Clure Strait. Tentative age considerations for these youngest lineations indicate the first evidence for an analogous extensive ice shelf configuration for the Last Glacial Maximum.

KEYWORDS
3D seismic data, Canadian Beaufort Sea, ice shelf grounding, Last Glacial Maximum, mega-scale glacial lineations

1 | INTRODUCTION

The glacial history of the Arctic Ocean is a topic of interest to Quaternary scientists, oceanographers, and environmental scientists who are studying glacial–interglacial cycles, ice shelf dynamics, and associated seabed processes (e.g., Engels et al., 2008; Grosswald & Hughes, 2008; Jakobsson et al., 2014; Niessen et al., 2013; Polyak et al., 2001). This topic also has relevance to those studying the interconnections between the ocean and the atmosphere during glacial times (e.g., Johnson & Andrews, 1986) and the effects of ice shelves influencing glacial flow dynamics at the margins of continental glaciers (Scambos et al., 2004). The concept of ice shelves and glacial ice cover

in the Arctic Ocean, including the possibility of a pan-Arctic ice shelf, was originally introduced on conceptual grounds drawing extensively on comparisons with modern ice shelves in Antarctica (Denton & Hughes, 1983; Mercer, 1970). More recently, marine geophysical and geological surveys from various regions of the Arctic Ocean have documented a variety of seabed features, including parallel grooves, that have been interpreted to be caused by the grounding of ice sheets or the grounding of the keels of ice shelves or icebergs (e.g., Engels et al., 2008; Jakobsson et al., 2005, 2010, 2014; Niessen et al., 2013; Polyak et al., 2001).

Mega-scale glacial lineations (MSGLs) were first described in the literature by Clark (1993) who reported large-scale streamlined lineations on previously glaciated terrain in northern Canada. He described parallel lineations 8 to 70 km long and 200 to 1300 m wide that were interpreted to form as a result of rapid glacial ice flow. A number of researchers studying active glacial processes in Antarctica have found that MSGLs are associated with ice streams and that they can also be formed at the base of grounded ice shelves in the offshore realm (Dowdeswell et al., 2007, and references cited therein; King et al., 2009). The classic MSGLs (on terrestrial or marine settings) are considered to be a subglacial bedforms associated with grounded ice streams, and are typically regarded as positive relief features (i.e., ridges, Spagnolo et al., 2017). As summarized by Jakobsson et al. (2014), glacial-related lineations have also been identified at greater water depths (800 to > 1000 m) on topographic highs in the Arctic Ocean. It remains a debate if these features should be called MSGLs, since they were probably formed beneath an ice shelf and therefore do not represent the same environment or conditions of a grounded ice stream. Nonetheless, the orientation of these lineations is significant for indicating the flow direction of a grounded ice mass. The presence of glacial lineations on topographic highs in the Arctic Ocean (e.g., Engels et al., 2008; Dowdeswell et al., 2010) raises the intriguing possibility that at least some parts of the Arctic Ocean were covered by vast and interconnected ice shelves (e.g., Jakobsson et al., 2010). However, as summarized in the review by Jakobsson et al. (2014), there remain many unanswered questions:

- Were ice shelves in the Arctic Ocean interconnected?
- Were there multiple ice shelves during past glacial cycles, or did these features exist only during the penultimate glacial maximum (Marine Isotope Stage [MIS] 6, Jakobsson et al., 2010)?
- How are the ice shelves fed by continental glacial sources?

We present geophysical interpretations of buried lineations, which are similar in character to MSGLs, from the outer continental shelf and upper slope of the Canadian Beaufort Sea, offshore of the Tuktoyaktuk Peninsula (Figure 1). While the majority of investigations of glacial lineations described in the literature are based on interpretations of seabed features identified in multibeam bathymetry or shallow high-resolution seismic imaging (e.g., Bellwald et al., 2018, 2019; Tasianas et al., 2016), we rely primarily on two-dimensional (2D) and three-dimensional (3D) multichannel seismic data to identify sub-seabed features. Two 3D seismic data volumes (informally named Ajurak and Pokak) provided to the Geological Survey of Canada by industry partners provide the basis for the main interpretations. Additional insights were derived from newly acquired 2D seismic surveys and hull mounted 3.5 kHz sub-bottom profiler sonars conducted by the Korean Polar Research Institute (Jin et al., 2015; Jin & Dallimore, 2016). Within the uppermost 400 m of marine sediments beneath the upper slope we have mapped three buried lineated surfaces at different stratigraphic levels. A previous examination of the industry 3D data set, conducted to assess seabed geohazards, identified two of these horizons which were considered to contain glacial-related lineations (Woodworth-Lynas et al., 2016a, 2016b). These lineations were interpreted to have been formed by seabed scour from a possible melange of icebergs and thick sea ice moving in a southwest direction. They are inferred to have formed during the last glaciation, with an estimated age of 19 to 16 ka based on extrapolated carbon-14 (^{14}C) ages documented in the reports. We seek to examine these features and another deeper lineated horizon in greater detail by documenting their morphology and geophysical characteristics as well as considering the age of the features. Our interpretations broaden the expanse of regional observations of glacially produced seabed lineations observed elsewhere in the Arctic Ocean (e.g., Jakobsson et al., 2010, 2014, 2016), and provide evidence for their source of glacial ice from the western Canadian Arctic Archipelago.

2 | BACKGROUND

Assuming that the buried lineations we describe are of a glacial origin, a brief review of the present understanding of the glacial history of the Beaufort Shelf and onshore areas of north-western Canada and Alaska is warranted. Regional Quaternary geology mapping efforts have been conducted over the past 50 years by the Canadian and American Geological Surveys and by a variety of university scientists. These studies suggest multiple Quaternary glaciations affected the Beaufort coast in Canada. Mapping efforts summarized in Rampton (1982, 1988) document that the maximum extent of the Laurentide Ice Sheet during MIS 2 (the Last Glacial Maximum [LGM]) only reached Herschel Island, and that the coastal areas further west, including northern Alaska, were unglaciated. Rampton's mapping did infer, however, that in order for glacial ice to reach Herschel Island, at least part of the Beaufort continental shelf adjacent to the coast must have been ice covered. The ice on the shelf was thought to have flowed out from the Mackenzie Trough, covering part of the Yukon Shelf and extending locally to areas northwest of Richards Island (Batchelor et al., 2013b). Quaternary mappers working in the western Arctic Islands have documented glacial sediments and landforms in this area that resulted mainly from flow from the north-western extension of the Laurentide Ice Sheet and contributions from the Innuitian Ice Sheet located in the high Arctic islands (Dyke, 2004; Dyke et al., 2002, 2003; England et al., 2006; Vaughan et al., 2014; Vincent, 1983). These researchers recognised westerly ice flow into Amundsen and M'Clure Straits (Figure 1) and suggested that at least some of the Beaufort continental shelf immediately offshore must have been glaciated. Perhaps the most contentious issue arising from the terrestrial mapping to date has been assigning the age of the glacial sediments and establishing if the ice was cold or warm based. The present consensus is that the late Wisconsin (MIS 2) ice cover was the most extensive in this area and that at least parts of the ice sheet were cold based (England et al., 2006). However, streamlined features (drumlin fields, dispersal trains and lineations) adjacent to many of the inlets on Victoria and Banks Island suggest episodic ice streams and

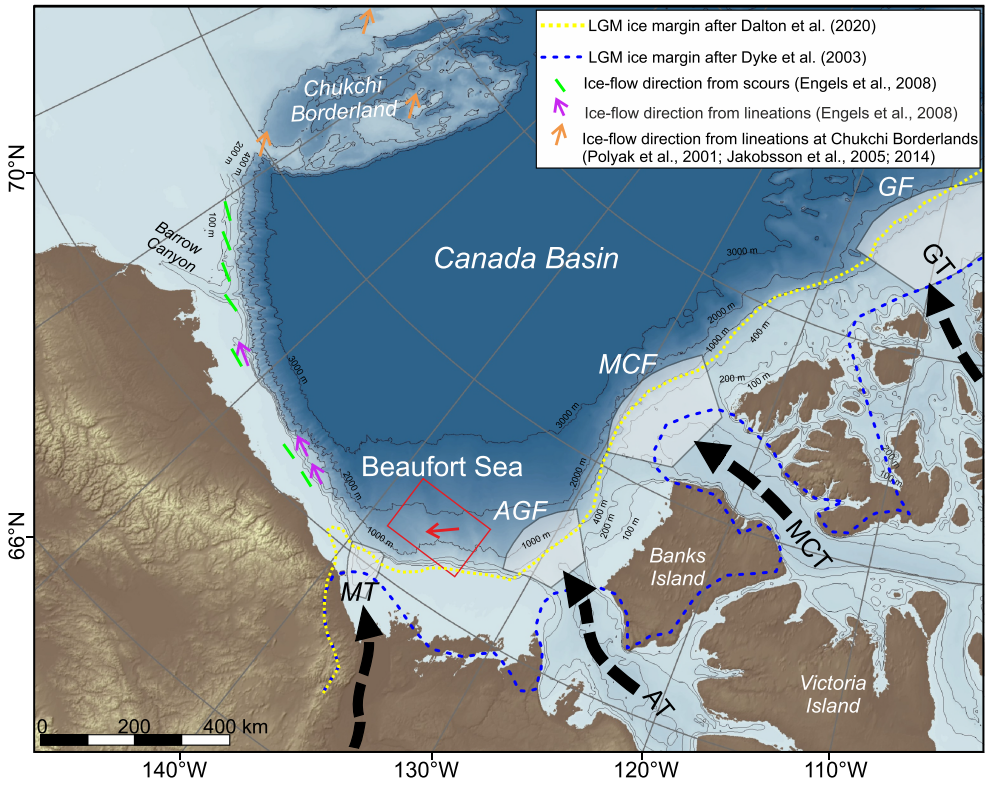

FIGURE 1 Map showing compilation of glacial limits and features associated with continental glaciation of North America during the Last Glacial Maximum (LGM) after Batchelor et al. (2019) and Dalton et al. (2020). Inferred ice-flow direction based on seabed lineations from studies in northern Alaska as well as at the Chukchi Borderland are also shown. Our newly inferred direction of ice flow is indicated by the red arrow. The red box marks our study region. Bathymetry is from the International Bathymetric Chart of the Ocean (IBCAO) V3 (Jakobsson et al., 2012) (MT, Mackenzie Trough; AT/AGF, Amundsen Trough/Gulf Fan; MCT/F, M'Clure Trough/Fan; GT/F, Gustav Adolf Trough/Fan) [Color figure can be viewed at wileyonlinelibrary.com]

ice shelves during deglaciation (e.g., Dyke, 2008; Hodgson, 1994; Stokes et al., 2005).

The assessment of the geology of offshore areas of the Canadian Beaufort Sea has benefited from industrial activities undertaken to evaluate the hydrocarbon potential of the area. Extensive regional multichannel seismic surveys have been conducted along the entire margin of the eastern Beaufort Sea and many geotechnical coring and site survey studies have been carried out at proposed exploration well sites. Using regional 2D seismic lines, Batchelor et al. (2013a, 2013b, 2014, 2016) interpret the presence of thick glacial tills in the Mackenzie Trough where Rampton inferred ice cover. They also document extensive trough mouth fans of glacial origin that extend onto the continental slope from M'Clure and Amundsen Troughs. Streamlined seabed features in the M'Clure and Amundsen Gulf also confirm ice movement from these Straits onto the continental shelf during the LGM (Blasco et al., 1990; MacLean et al., 2010, 2016; Niessen et al., 2010; Stokes et al., 2005, 2006). However, the regional 2D seismic data sets reveal no indication of glacial tills or thick glaciogenic sediment assemblages elsewhere on the continental shelf. Similarly, we are unaware of any observations of glacial tills in deep geotechnical core holes completed on the continental shelf by industry (more than 100 industry reports are available through the Arctic Science and Technology Information System, available online at http://www.aina.ucalgary.ca/astis/).

However, despite the limited evidence in the offshore Beaufort Sea margin, Dalton et al. (2020) have suggested revision of the glacial map of North America that extends broad ice cover to the continental shelf edge from the Arctic Islands in the east to the northern Yukon during the LGM (yellow dotted line in Figure 1). A recent synthesis of empirical and modelled evidence for the extent of Northern Hemisphere ice sheets through the Quaternary carried out by Batchelor et al. (2019) also suggests the possibility of extensive ice cover on the continental shelf along the Beaufort Sea margin (including our study region of Tuktoyaktuk peninsula, see figure 1d by Batchelor et al., 2019) and the existence of successive ice streams in the Amundsen Gulf/M'Clure Strait region during several Quaternary glacial periods. Evidence of multiple early to mid-Pleistocene glaciations has been described from coastal sections along the Beaufort Sea (Barendregt et al., 1998; Carter et al., 1988; MacCarthy, 1958; Vincent, 1990; Vincent et al., 1984). However, uncertainty arises due to limited exposure of these older sediments and concerns that glacio-tectonism caused by late Wisconsin ice cover could have disrupted the sediment assemblages and assigned dates (Vaughan et al., 2014).

3 | DATA AND SEISMIC ATTRIBUTE CALCULATIONS

In this study we utilize two 3D seismic data volumes provided by industry as well as newly acquired 2D multichannel seismic (MCS) and sub-bottom profiler data collected using the Korea Polar Research Institute (KOPRI) icebreaker ARAON in 2014. The location of the seismic data sets together with detailed bathymetry is shown in Figure 2. The industry 3D seismic data were provided as pre-stack time-migrated sections and processing included (in addition to 3D geometry definition), cable depth datum correction, de-bubble phasing designature deconvolution, low-cut filtering, swell-noise attenuation, direct arrival attenuation, channel amplitude correction, water column statics, common-offset noise attenuation, Q-compensation (phase only), high-resolution radon de-multiple processing and anisotropic pre-stack migration. Additional care was taken to suppress the acquisition footprint (in this case predominantly east–west [E–W] oriented). The 3D seismic data were further processed by the Geological Survey

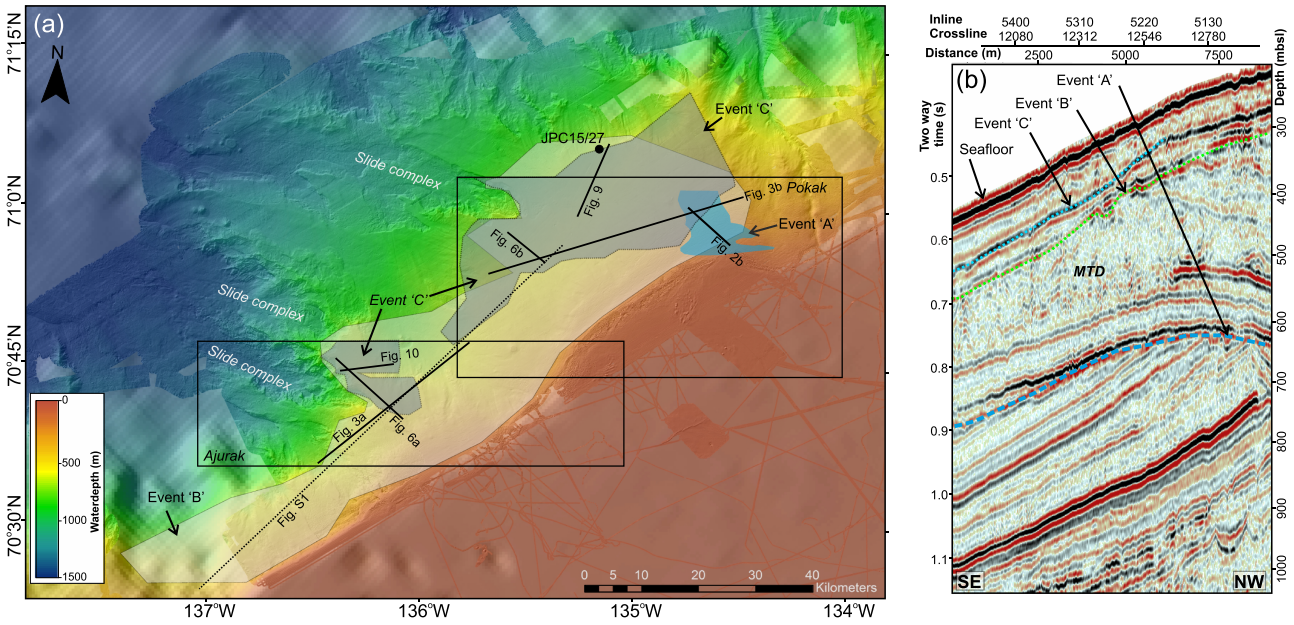

FIGURE 2 (a) Bathymetric map of the study region showing extent of the three identified events with large-scale glacial lineations. Oldest 'event A' (light blue area) is preserved over only a small portion in the eastern study region, 'event B' (light grey area) is seen across most of the study area, and the youngest 'event C' (dark grey area) coincides with much of the area of 'event B'. All seismic lines used in this study are marked as solid black lines and the outline of the two three-dimensional (3D) seismic data volumes Ajurak and Pokak are shown as black rectangles. A seismic section (re-digitized from an analogue paper-record) crossing the study area is shown in the Supporting Information Figure S1 (dotted line). (b) Type section of seismic data extracted from Pokak 3D volume showing a setting with all three identified events with glacial lineations [Color figure can be viewed at wileyonlinelibrary.com]

of Canada (GSC) using the similarity attribute (also referred to as coherency attribute) to enhance imaging of structural discontinuities such as faults, channels and the glacial mega-lineations. The similarity attribute is computed as semblance using a range of one neighbouring trace around each input-trace, a 20 ms vertical time window, and within a frequency range of 8 to 80 Hz. Several horizons were derived by manually picking events from the time-migrated 3D seismic data inside a seismic interpretation software package, and exported for further statistical analysis performed inside ArcGIS.

The KOPRI 2D MCS survey used an airgun array of 1200 in^3 volume and a streamer with 120 channels with maximum offset of 1600 m (Riedel et al., 2016). Seismic data were processed (after crooked-line 2D geometry definition) using a sequence including removal of DC offset, muting of direct arrivals and refractions, minimum phase band-pass filtering, surface-consistent deconvolution, stacking-velocity definition using the semblance technique, staking (full-offset range) and post-stack Kirchhoff time migration using a 2D variable velocity field. Details of the processing and interpretation of these 2D MCS data are given in Riedel et al. (2016). The MCS data have been used previously to define interval velocities (Riedel et al., 2016) and we use these velocity–depth functions to convert observations on the 2D and 3D data made in two-way travel time to depth (metres below seafloor, mbsf). The uncertainty in this conversion depends on water-depth and burial depth below seafloor and is practically a measure of robustness of the P-wave velocity–depth functions defined from the MCS data. As described in Riedel et al. (2016), the P-wave interval velocity function is well established in water depths exceeding ~300 m but is complicated and laterally fast-changing near the continental shelf edge with rough topography and across most of the continental shelf region due to shallow-water multiples. In the analyses described later, our measurements of lineation depth and width are associated with an additional (individually ascribed) uncertainty based on sample-rate (vertical extent) and 3D bin-size (lateral extent).

4 | REGIONAL SEISMIC STRATIGRAPHY

Seismic data and stratigraphic information obtained from historical hydrocarbon exploration programmes provide a comprehensive basis to characterize the regional Cenozoic stratigraphy of the Beaufort–Mackenzie Basin (e.g., Dixon, 1996; Dixon & Dietrich, 1990; Dixon et al., 1992; McNeil et al., 2001). The upper-most sedimentary sequence (upper 2–4 km) of the offshore record has been classified into two depositional formations: the Iperk Formation (early Pliocene to mid Pleistocene age) and the Shallow Bay Formation (mid Pleistocene to Holocene age). While the data sources are sparse, especially on the outer continental shelf, a regional angular unconformity associated with the base of the Iperk Sequence is thought to be prominent in the study area (e.g., Dietrich et al., 2010) at 2.0–2.5 s two-way time on regional seismic data (equivalent to a depth of 2.8 to 3 km below seafloor). The base of the Iperk Sequence is deeper than the available 3D seismic data sets we have accessed. The Shallow Bay Formation above the Iperk includes glacial erosion across parts of the continental shelf and was defined by Dietrich et al. (1985) in the Mackenzie Trough using a seismic reflection line; it was later interpreted to occur on the slope tens of kilometres away on a reflection profile (Dietrich et al., 2010) acquired in 1987 as part of the Frontier Geoscience Programme (FGP) some distance west of our study site (e.g., Dietrich et al., 1989). Our interpretations derived from the 3D seismic data

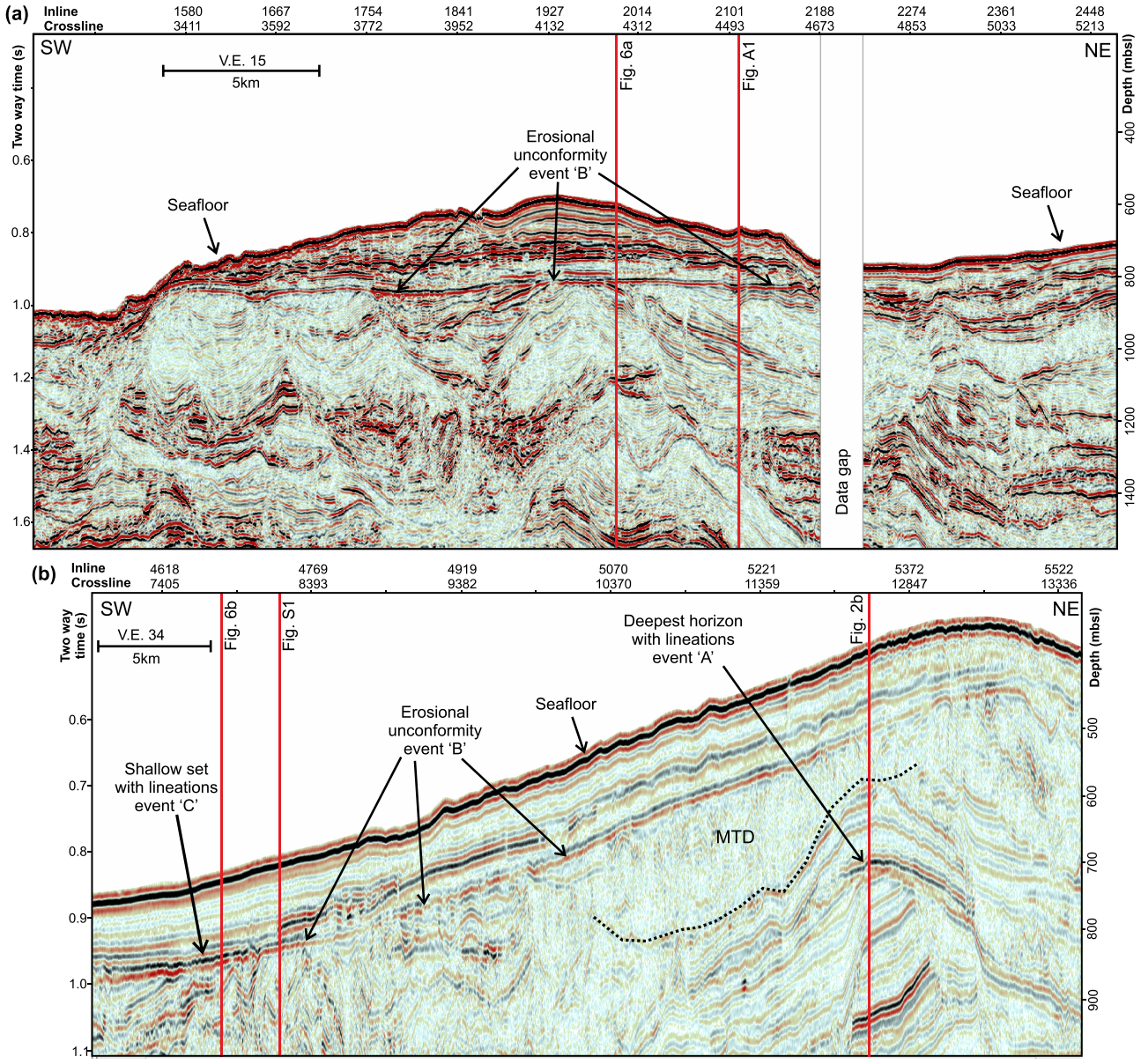

FIGURE 3 (a) Seismic section extracted from the Ajurak three-dimensional (3D) seismic volume highlighting the uppermost erosional unconformity 'event B'. (b) Seismic section extracted from the Pokak 3D seismic volume showing the erosional unconformities 'A' and 'B', and 'event C', as well as other large-scale depositional features common in this region such as mass-transport deposits (MTDs). Locations of seismic sections see Figure 2 [Color figure can be viewed at wileyonlinelibrary.com]

sets provide new insights into the seismic stratigraphy of the study area. The geology imaged in the upper 2–3 km is complex and marked by thick channel-levee complexes, numerous angular unconformities and distinct packages of sediments which display a broad range of soft sediment deformation structures and mass transport deposits (Rohr et al., 2021, Figure 3). These include coherent slide blocks and debris flow deposits and deformation as localized normal faults and slump features. These features are indicative of rapid sediment deposition in a slope fan environment. Two slope fans have coalesced; they appear to have originated from fluvial systems that predate formation of the present Mackenzie River system during the LGM (Duk-Rodkin & Hughes, 1994; Rohr et al., 2021). The slope fans have been regionally truncated by a shallow planar erosional unconformity which is overlain mainly by horizontally laminated sediments (Figure 3 and Supporting Information Figure S1). This unconformity represents a significant change in depositional style from an environment associated with rapid deposition and sediment deformation within the slope fan (Rohr et al., 2021), to glacially-dominated erosion and deposition cycles. This slope-fan environment would have been the site of significant meltwater runoff during several Quaternary deglacial events. The slope fans are morphologically distinct from the glacially influenced Amundsen Gulf and M'Clure Strait trough mouth fans described by Batchelor et al. (2013b, 2014).

5 | RESULTS: CHARACTERISTICS OF OBSERVED LINEATIONS

Using the 3D seismic attribute similarity, we scanned the 3D seismic surveys in our study area for events with potential lineations, especially those associated with angular unconformities. Within the uppermost 0.9 s two-way time, or 0.54 s below seafloor, we have identified

three buried lineated horizons (Figure 2) which have similar morphology to other glacial lineations reported in the Arctic (e.g., Engels et al., 2008; Jakobsson et al., 2005, 2010, 2014, 2016; Polyak et al., 2001). The character of the lineated surfaces is described in the following sections. Here, we interpret the lineations as predominantly negative relief features (grooves) rather than positive relief ridges. Representative examples of profiles across each horizon are included in the results shown below and more extensive examples and analyses are given in the Supporting Information. All of the lineated surfaces we observe have significant sediment cover and therefore have limited expression on the present seabed. This is in contrast to other lineations described in the Arctic that have only shallow burial depths and can therefore be identified on multibeam or side scan imagery (e.g., Engels et al., 2008; Jakobsson et al., 2005, 2010, 2016). This reflects our location within the principal Cenozoic depocentre of the Beaufort–Mackenzie Basin with high post-glacial sedimentation rates.

5.1 | Oldest (deepest) lineated 'event A'

The deepest reflection event (unconformity) associated with lineations occurs between approximately 0.8 and 0.9 s two-way time (~275–390 mbsf, and ~600–750 m below present sea level) within the Pokak 3D volume (Figure 4). The unconformity, which occurs within the upper part of a bedded channel-levee complex described by Rohr et al. (2021), has varying dip angles and topography. It has been eroded in many parts of the study area and as a consequence is only approximately 180 km^2 in area. A total of 343 individual lineations have been mapped on this surface (Figure 4) with most trending at an orientation of 45°, and a small subset oriented at ~35°. The lineations are negative relief features, i.e., grooves (Figure 4f). The length of the individual grooves varies between 200 m and 1800 m with a mean of 590 m. Shorter segments are difficult to define because the signal to noise-level is relatively low in this part of the seismic data.

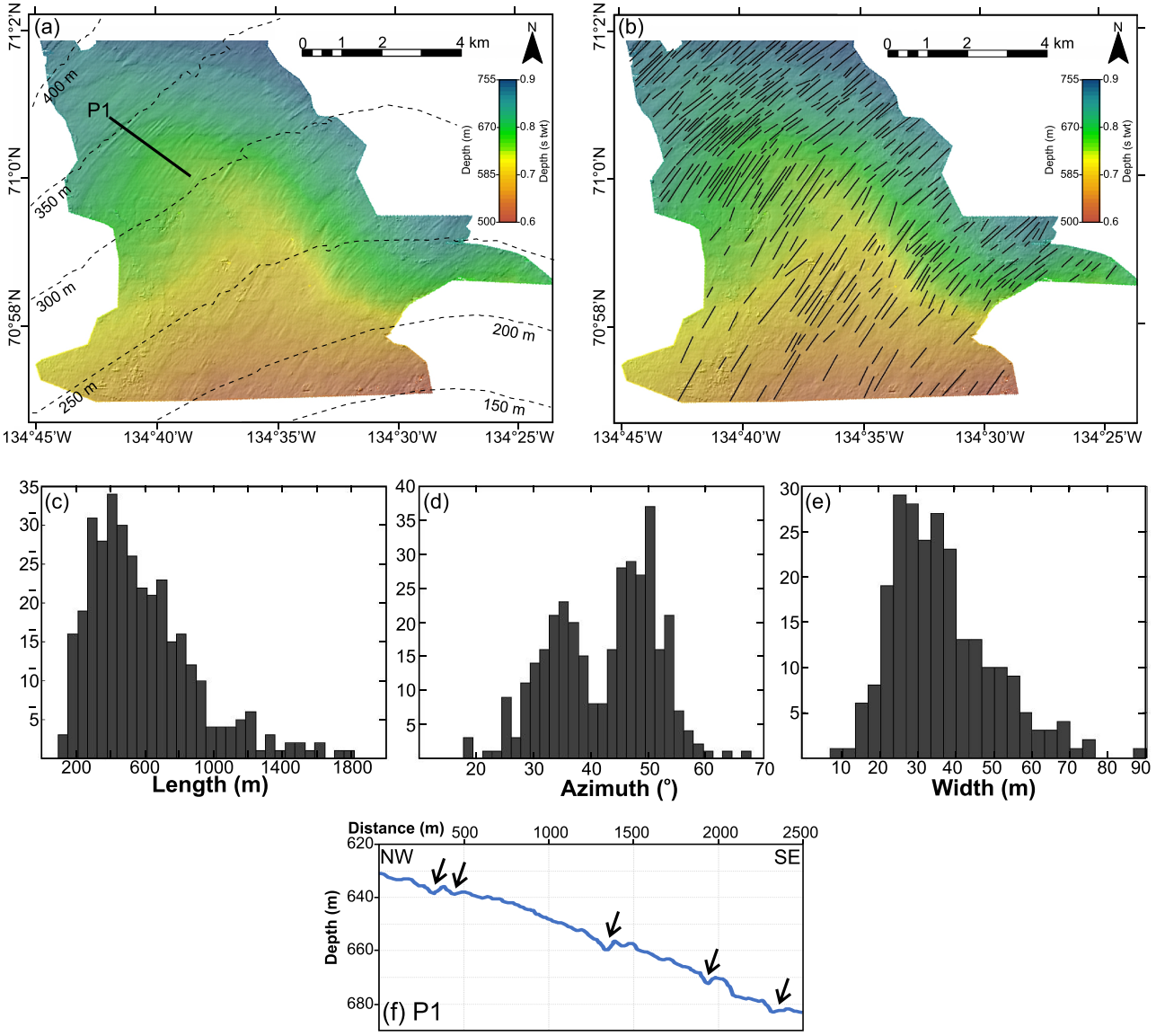

FIGURE 4 Maps showing (a) topography of 'event A' extracted from Pokak three-dimensional (3D) seismic data volume (underlain by hill-shaded relief illuminated from 315°), (b) digitized individual lineations across this horizon, with corresponding histogram distribution of (c) length, (d) azimuth, and (e) width of the lineations. Contour-lines in (a) are present-day water depth. The seismic horizon surface is shown in depth of seconds two-way travel time (s twt) as well as metres below sea surface. (f) Depth-profile of P1 defining the lineations as negative-relief feature (black arrows) [Color figure can be viewed at wileyonlinelibrary.com]

TABLE 1 Width of the grooves derived from surfaces across the two three-dimensional seismic surveys Ajurak and Pokak

		Event B				Event C			
	Event A	Ajurak	Pokak (all)	Pokak (west)	Pokak (east)	Ajurak	Pokak (all)	Pokak (west)	Pokak (east)
Mean (m)	37	60	68	66	72	73	46	50	42
Median (m)	34	51	66	62	72	60	37	41	34

The width of the grooves (mean of 37 m, Table 1) is therefore determined with a lower cutoff value of ~10 m, with the 3D data being actually on a 6.25 m (E–W) by 12.5 m (north–south [N–S]) spacing. The histograms for width and length are skewed towards lower values (as is also observed for similar bedforms by Spagnolo et al. [2014, 2017]), which may be a result of the threshold given by the gridding of the data. Beds within ~0.1 s two-way time (or ~80 m) above the unconformity drape the lineations but gradually become flattened above. The sequence is then truncated and partially eroded by a massive mass-transport complex associated with channel levee deposits.

5.2 | Lineated 'event B'

Lineated surface 'B' is associated with a wide-spread erosional unconformity that occurs within the upper-most 0.2–0.3 s two-way time below seafloor (~160–240 mbsf, using a velocity of 1600 m/s). This unconformity is observed on all available 2D and 3D seismic data sets on the slope region of the study area, except where active slope failures post-dating the event have removed it along with much deeper sediments. It was mapped across a total area of ~3150 km^2. The erosional surface is relatively smooth and planar (Figures 2, 3 and S1) on a regional scale. The interval between the unconformity and the seafloor consists of mostly layered sediments that were initially deposited parallel to the unconformity (Figure 3). The deep-water extent of the unconformity is limited by the occurrence of large coalesced slide complexes, which have removed the horizon and much of the sediment both above and below it. The offshore extent of the lineated surface is defined at present water depths of 600 to 880 m while the unconformity itself appears to pinch out at the continental shelf edge in current water depths of ~150 m.

The lineated surface 'B' is very well imaged on the seismic data sets and the lineations are up to 6 km in length and arranged parallel to one another. As shown in Figures 5 and S2, two sets of parallel lineations occur at dominant orientations of 55° to 59° close to the continental shelf break in the eastern study area, and 46°–48° in deeper water to the west. The lineations are mainly U-shaped and asymmetric with small ridges on each side (Figure 5c, d). These grooves are relatively shallow with depths of 2 to 5 m (measured at the deepest point of the depression; uncertainty of depth calculation is ~0.5 m). The width of the grooves varies along the surface of the two 3D data sets, but the majority of the lineations are less than 150 m wide (uncertainty of width is on average 10 m as per 3D seismic data bin size). Using the extracted surfaces, a comparison of groove azimuth and width across the entire region where they are preserved can be made (Figure 5f). Comparing the widths of the grooves over Ajurak and Pokak shows that they may progressively narrow towards the southwest with an increase in the average distance between grooves (i.e., ridge-widening) towards the west (Figure 5f). Sometimes, several grooves occur within a wider depression. In these cases, width was then defined for the individual thinner and the combined wider groove. We also note that multiple grooves commonly merge into one larger feature towards the southwest. However, groove depth is highly irregular along the surface with grooves deepening and shallowing several times along their paths (up to 30 km in length across the Pokak region) and no consistent depth-trend is observed (see also Supporting Information Figure S4). Unlike the sediments which occur above lineated surface 'A', the sediments bedding above surface 'B' do not appear to mimic the groove geometry.

5.3 | Lineated 'event C'

Lineated 'event C' (Horizon 5 of Woodworth-Lynas et al., 2016b) occurs in close proximity to surface 'B', generally within 0.05 s two-way travel time or ~40 m (Figure 6). The individual lineations of surface 'C' can be discriminated on the seismic data as a separate event and do not coincide spatially with those of 'event B' (i.e., they are not simply filled older lineations). To capture a detailed and unbiased trace of the lineations in the 3D seismic data, a continuous, coherent basal reflector of the overlying stratified unit was mapped; the actual 'target' surface is likely just below this, at the top of the chaotic to homogeneous unit. This yields a faithful manifestation of the grooves because of the near-perfect conformability (mimicking). Accordingly, the surface of 'event C' itself is a disconformity, contrasting with the unconformity of 'event B'. Sediment layers deposited above 'event C' are well stratified, mimicking the underlying grooves and ridges, to the degree that the seabed locally retains this fabric. Exceptions are where subsequent mass transport events have occurred. Where preserved, the lineations on 'event C' occur at depths of ~40 to ~140 mbsf (across Ajurak) and ~125 m (across Pokak) and present-day water depths from 650 to ~800 m. Mapping of the surface using 3D, 2D seismic, and high resolution sub-bottom profiler data reveals that in present-day water depths of > 500 m the surface with lineations can be observed along the margin for up to 56 km in length with near-constant groove-orientation between 43° and 45° (Table 1). A progressive change in azimuth following the slope topography is seen in shallower water across the Pokak area (similar to unconformity 'B') with a maximum azimuth of 70° in water depth of ~360 m (Figure 7 and S3). The average distance between lineations is apparently less in shallower water depths. The orientation of the lineations is similar in character to those on unconformity 'B'; however, several grooves are much deeper (up to 15 m) than those seen on the unconformity 'B'. The surface area of 'event C' preserved across Ajurak is less than in the Pokak area and thus the statistics derived in this area are less robust. However, the groove widths appear wider at Ajurak than at Pokak (compare to Supporting Information Figures S4 and S5).

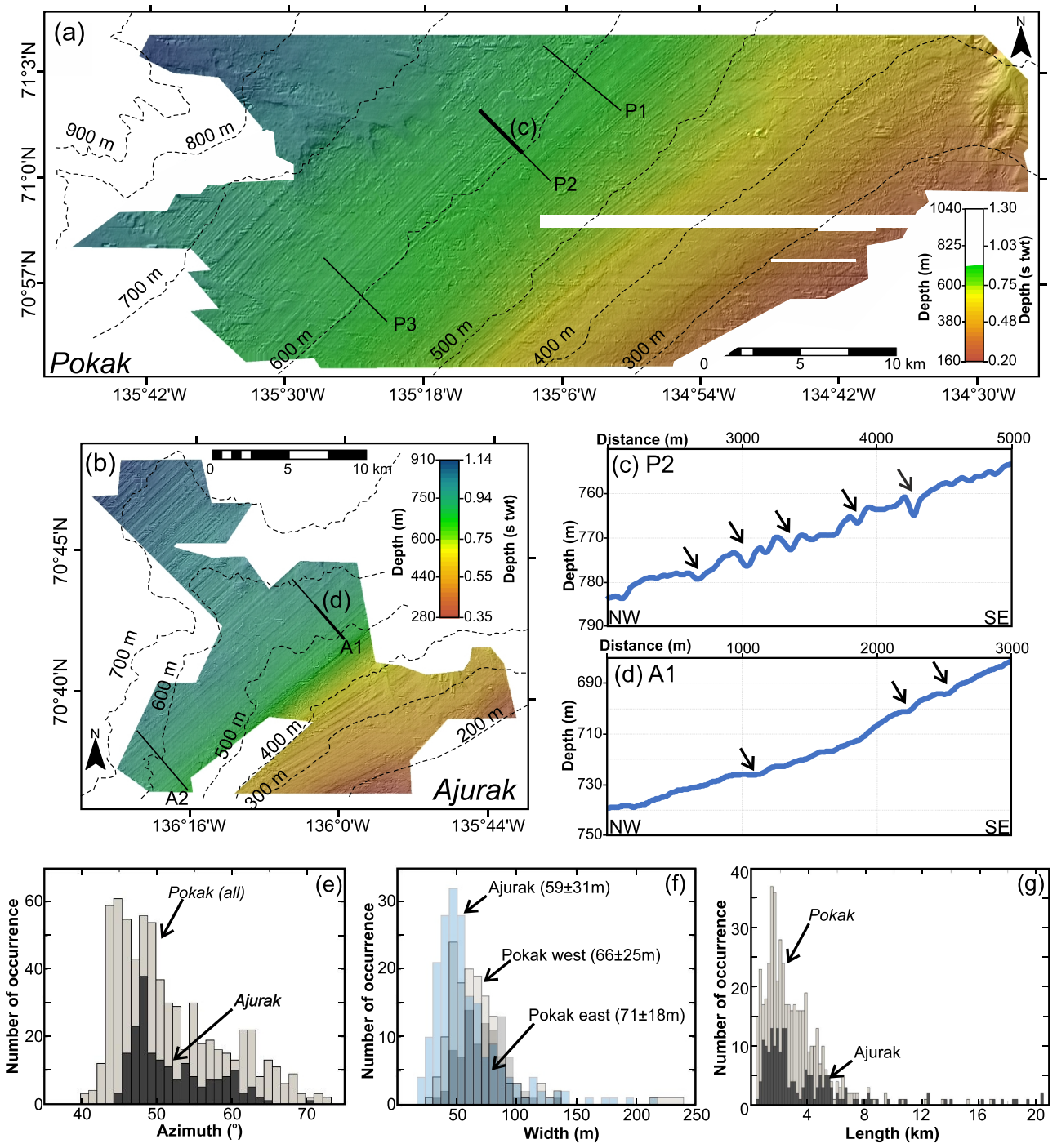

FIGURE 5 Maps showing topography of surfaces corresponding to 'event B' extracted from (a) Pokak and (b) Ajurak three-dimensional (3D) seismic data volumes (digitized lineations see Supporting Information Figure S2). Contour-lines in (a) and (b) are present-day water depth. The seismic horizon surface is shown in total depth of seconds two-way travel time (s twt) as well as metres using a velocity of 1600 m/s for conversion. Portions of the profiles P2 and A1 are shown in (c) and (d), respectively, demonstrating the lineations as negative relief features (grooves). Examples of prominent depressions are indicated by black arrows. All five topographic cross-profiles (P1–P3, A1–A2) are shown in Supporting Information Figure S4. (e)–(g) Histogram distributions of groove statistics for azimuth, width, and length, respectively. The 3D data coverage is irregular, skewing the statistic towards non-representative lower cutoff values [Color figure can be viewed at wileyonlinelibrary.com]

The width measurements refer to the actual grooves; inter-groove spacing frequency distribution is presented in the Supporting Information. It shows a dominance at just under 1000 m spacing, with no examples exceeding this, and a gradual frequency of occurrence trailing to 100 m spacing. The metrics for MSGLs produced beneath a grounded ice stream presented with their original recognition (Clark, 1993) and newer observations (e.g., Livingstone et al., 2016; Spagnolo et al., 2014) indicated a normal frequency distribution with spacing centred about 4000 m. Our measured lengths are significantly shorter, several kilometres *versus* tens of kilometres, but both their area of preservation and data extent are strong limiting constraints. Nevertheless, numerous studies addressing MSGL scale also include a spacing range overlapping ours (e.g., Cofaigh et al., 2016; Dowdeswell et al., 2016; Ely et al., 2016; King et al., 2009).

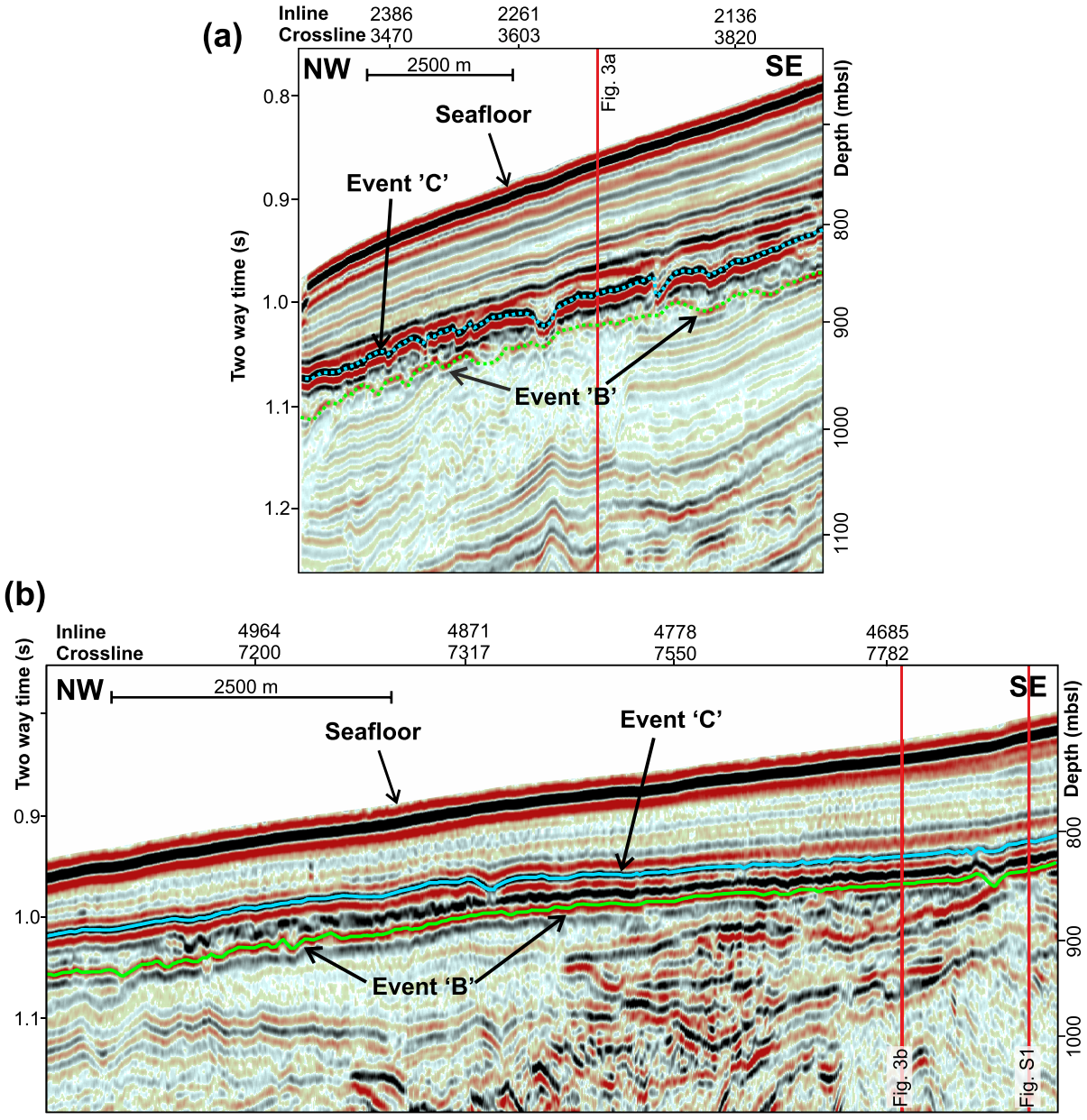

FIGURE 6 Examples of seismic sections showing the erosional unconformity 'event B' (light blue line) and the 'event C' (green line) extracted from (a) Ajurak volume and (b) Pokak volume. Location of lines see Figure 2 [Color figure can be viewed at wileyonlinelibrary.com]

6 | DISCUSSION

6.1 | Genesis of lineations

The three seismic reflection events with lineations we document each have striking similarities to glacial lineations described in other marine environments, such as reviewed by Dowdeswell et al. (2007), Rafaelsen et al. (2002), and Jakobsson et al. (2016). While orientations in our data set vary somewhat, all of the lineations align approximately in a northeast–southwest direction and they follow the slope contours (see 3D surface rendering in Supporting Information Figure S7). While principally developed across smooth and near-horizontal to gently dipping planes, the lineation character varies somewhat depending on the slope geometry on which they have formed. The widespread extent of the lineations (100–150 km^2), length of individual lineations (commonly > 3 km long), their consistent and common orientation across large areas, and their self-similar morphology is consistent with formation by movement of contiguous ice across the seafloor. We can envision only a limited number of other possible origins for the lineations. The 3D seismic data allow us to assess the sediment layering above and below the lineated surfaces and we see no evidence that they could be produced by dipping sediment horizons outcropping on a paleo seafloor. The lineations are very linear and evenly spaced and not at all similar in scale or form to possible ancient shore line features or bedforms (e.g., sand ribbons or current furrows as described in Flood [1983]) resulting from current/wave action. The lineations also contrast with a much more random pattern of iceberg scoured (ploughmark) terrain (e.g., Woodworth-Lynas et al., 1985) which is clearly observed at the seabed along a > 500 km stretch of shelf break but restricted to shallower than

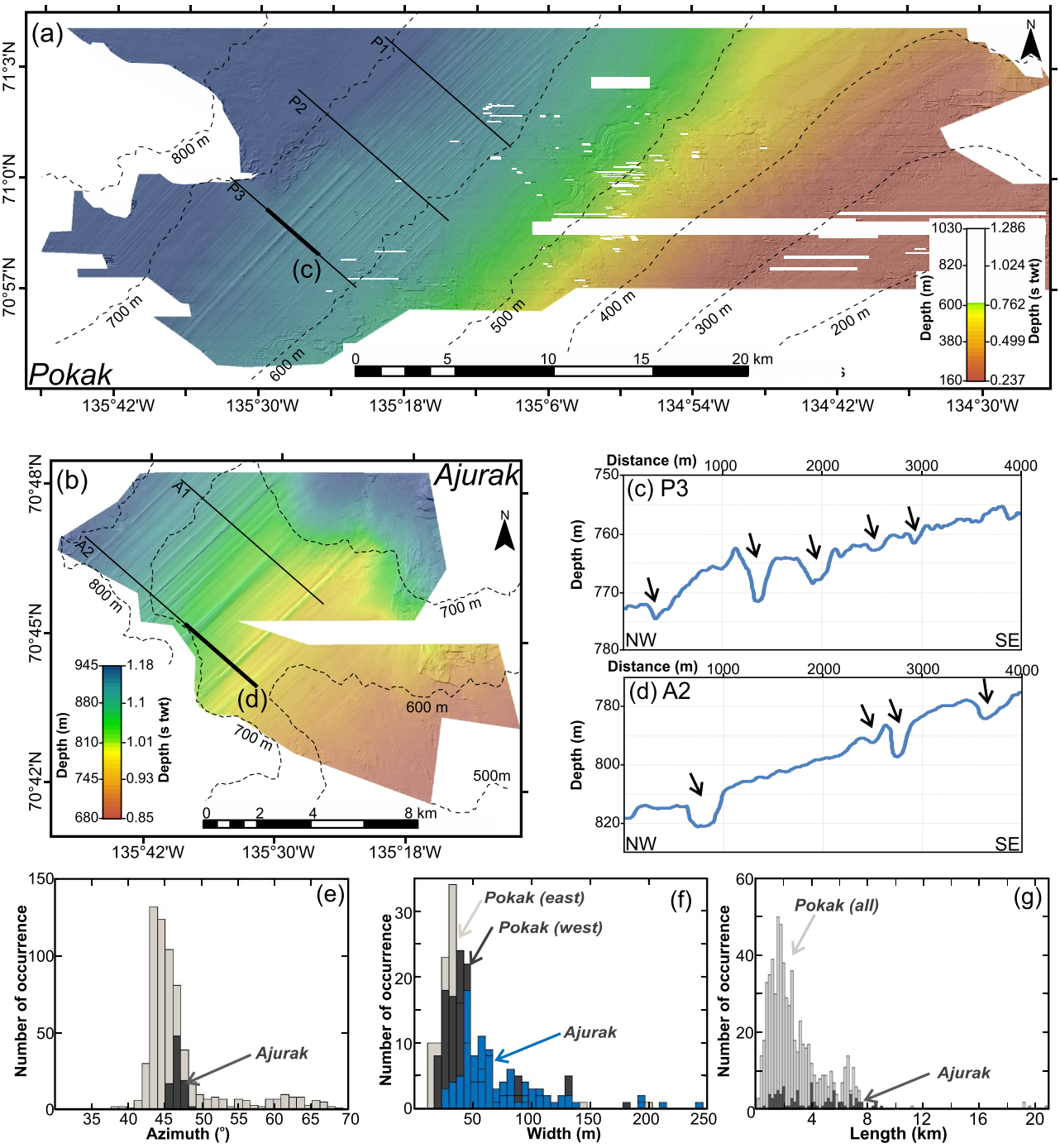

FIGURE 7 Maps showing topography of surfaces corresponding to 'event C' extracted from (a) Pokak three-dimensional (3D) and (b) Ajurak seismic data volumes (digitized lineations see Supporting Information Figure S3). Contour-lines in (a) and (b) are present-day water depth. The seismic horizon surface is shown in total depth of seconds two-way travel time (s twt) as well as metres using a velocity of 1600 m/s for conversion. Portions of the depth-profiles P2 and A1 are shown in (c) and (d), respectively, demonstrating the lineations as negative relief features (grooves). Examples of prominent depressions are indicated by black arrows. All five topographic cross-profiles (P1–P3, A1–A2) are shown in Supporting Information Figure S5. (e)–(g) Histogram distributions of groove statistics for azimuth, width, and length, respectively [Color figure can be viewed at wileyonlinelibrary.com]

~420 m water depths. Even considering iceberg scours buried by Holocene sediments in our study area reaching a maximum of 500 m present water depth is not congruent with the observed much deeper lineations.

While there is general agreement that MSGLs themselves are indicators of glacial flow direction, there is considerable discussion in the literature about their formation mechanism (e.g., Boulton & Clark, 1990; Canals et al., 2000; Clark et al., 2003; Cofaigh et al., 2005; Dowdeswell et al., 2007, 2010; Fowler, 2000, 2009; Hindmarsh, 1998; King et al., 2009; Shaw et al., 2008; Tulaczyk et al., 2001). Our analyses of the morphology of the lineated surfaces suggest that they are primarily negative relief features, or grooves, carved into the paleo-seafloor (Figures 4, 5 and 7). They typically have an asymmetric shape, with modest variability in distance between grooves and their depths, width and intervening ridge height. This suggests that the bed interactions were somewhat variable in time and space. Observation of the progression of morphology along the lineations demonstrates a growth and then diminishing in both depth

and width of the groove and also, but less commonly, building of an intervening ridge (Figures S4 and S5). Ridge volumes are less than those of the grooves, suggesting that their formation may be a more secondary process, that is, not strictly a function of displacement from the groove. This introduces the possibility that they could be molded by the ice in a dynamic interplay of erosion and re-deposition. We therefore suggest that the lineations seen on all three surfaces mapped are from a grounded ice mass and a groove-ploughing-type process. We also assign the term MSGL to our lineations as they are clearly representing large-scale glacial processes along the Beaufort margin and are similar in character to those features described elsewhere in the Arctic as reviewed by Jakobsson et al. (2016).

In addition to the MSGL features themselves, associated sediment characteristics such as evidence for erosion, deformation of bed materials, or sub-ice emplacement of glaciogenic sediments can be useful in the assessment of their origin. Assuming that the lineations we observed were formed by grounding of an ice mass in contact with the sea bottom, we conclude that the most definitive indicator of flow direction would be changes in groove character along the length of the feature. In uniform water depths, such is the case for most of our study area, it is possible that the grooving would become less sharp and well defined in the down flow direction as the resistive feature in the bed of the ice gradually erodes as it is dragged along the sea bottom (Figure 8). We have examined the grooved surfaces in the 3D data sets to consider if morphology of the lineations suggests the direction of ice-movement (Figures 7, 8, S4, S5 and S6). The most definitive conclusions can be drawn from the youngest 'event C' features. Event C grooves change significantly in dimension and abundance along their length with numerous narrow features in the Pokak area in the northeast and fewer more broad features in the Ajurak area in the southwest. This is consistent with a flow direction from the northeast to southwest, which would be consistent with ice flow originating from Amundsen Gulf and/or M'Clure Strait. The lineations on unconformity 'B' are rather uniform in morphology from the Ajurak to Pokak areas (Figure 5); however, as revealed for 'event C', the grooves in the southwest across Ajurak in comparable water depths to the Pokak region are somewhat wider and fewer grooves

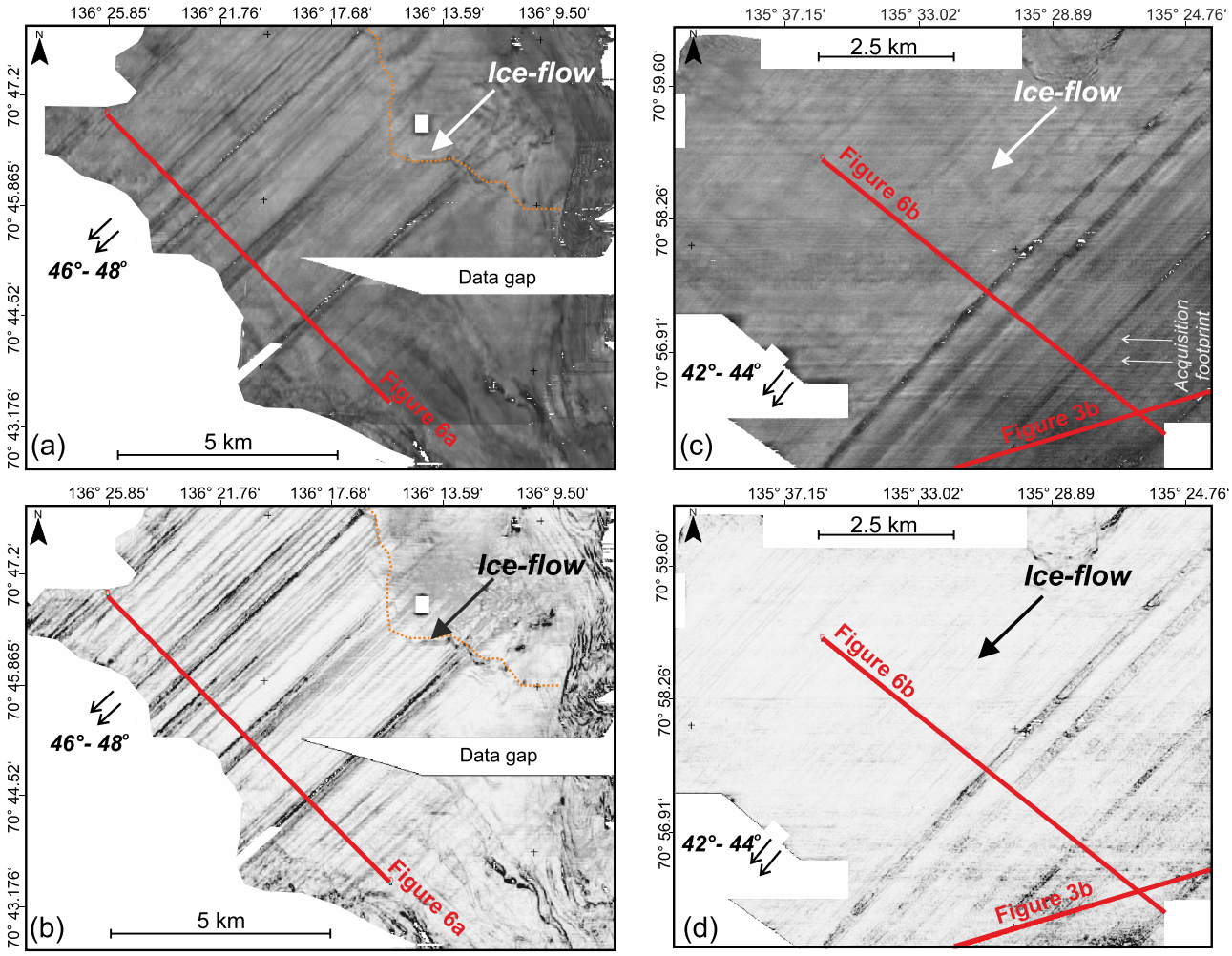

FIGURE 8 Time slices of 'event C' extracted from the Ajurak three-dimensional (3D) seismic data showing (a) reflection amplitude and (b) similarity attribute; same event extracted from the Pokak 3D data showing (c) reflection amplitude and (d) similarity attribute. The orange dotted line in (a) and (b) marks transition of the 'event C' from deeper (northeast, NE) to shallower (southwest, SW) water- and horizon-depth. Lineations are less developed across this sloped surface and can be traced only for 800 to 1400 m downslope. With shallowing, (NE to SW), lineations initiate as thin, shallow grooves that progressively deepen and widen. On reaching maximum topographic height, grooves continue but merge so that the overall depth of the groove increases as does their combined widths. Relief from initiation to maximum elevation is about 35 m. We infer ice-flow direction from NE to SW [Color figure can be viewed at wileyonlinelibrary.com]

are present along the same profile-distance than to the northeast across Pokak (Figure 5). Since both horizons are in close proximity to each other, it may be reasonable to assume a similar ice-movement direction for 'event B' as made with higher confidence for 'event C'. In contrast, the very limited spatial extent of the mapped lineations comprising 'event A' limits any rigorous evaluation and therefore interpretation of flow direction. Event A is further complicated as the orientation of the surface is more steeply dipping.

6.2 | Age of lineations

The absolute timing for the events that formed the three observed horizons with MSGL is challenging to assess as to date no sediment cores have been recovered from these horizons. However, extensive shallow coring has been conducted on the upper slope mainly for geohazard studies (Woodworth-Lynas et al., 2016a, 2016b) and recently, a ~17 m long stratigraphic core has been collected from the upper slope (Keigwin et al., 2018; Klotsko et al., 2019) in the eastern part of our study area (location of JPC 15/27 see Figure 2a). The long core is particularly helpful as it has been well dated enabling correlations to be made with high-resolution sub-bottom profiler data (i.e., figure 14 in Klotsko et al., 2019). A detailed correlation is given in Supporting Information Figure S8 between the acoustic data shown in Klotsko et al. (2019) and our database of sub-bottom profiler data (Blasco et al., 2013) and more recently acquired data with the icebreaker ARAON (Jin et al., 2015; Jin & Dallimore, 2016; Riedel et al., 2016). Correlations of the acoustic sub-bottom profiler data to the stratigraphic framework and ^{14}C ages were previously made by Woodworth-Lynas et al. (2016a) and King et al. (2017) and we expanded those to the data relevant to our study. Through these assessments we have determined that the main reflector horizons identified can be traced in the sub-bottom profiler data across the Pokak (Figure 9) and Ajurak (Figure 10) 3D survey areas. We have focussed on three distinctive seismic horizons as they can be correlated with a high degree of confidence to the Klotsko et al. (2019) assessment (see H2, H3, and H5 on Figures 9 and 10). This approach suggests that the deepest reflector H5 has an estimated age of ~18 ka. This horizon is above a layer with low acoustic reflectivity that is situated directly above lineated 'event C'. The character of this layer suggests a different depositional environment than the well laminated sediments above and may indicate a period of more rapid deposition, coarser grained sediments or even be indicative of emplacement of more heterogeneous glacial sediments. The age and environment of deposition of the thick (50–70 m) glacimarine and (thin) post-glacial succession of stratified sediments covering 'event C' is well established above horizons H3 and H5 (see references cited in Figure 10 caption). If the correlation of the acoustic and core data is reliable, the formation of 'event C' likely occurred somewhat before 18 ka and may be associated with the LGM. While 'event B' is quite distinct from 'event C', the close proximity of the horizons in the seismic section and their similar areal extent suggests that they are close in age and may indicate intermittent grounding of the ice during the last glacial cycle. While we cannot definitively assign the age of 'event B', we propose that 'event C' almost certainly formed during the LGM as the cover of mostly laminated sediments document a transition that is consistent with change from a grounded to floating ice environment (Klotsko et al., 2019). Given our recognition of a thick stratified post 'event C' deglacial sedimentary blanket containing no significant sediment disruption in combination with the thin homogenous unit between these two events, we infer a limited duration separating events B and C, likely not on the scale of glacial cycles. In, contrast, 'event A' (only preserved as an erosional remnant) occurs at considerably greater depth and with a different orientation and

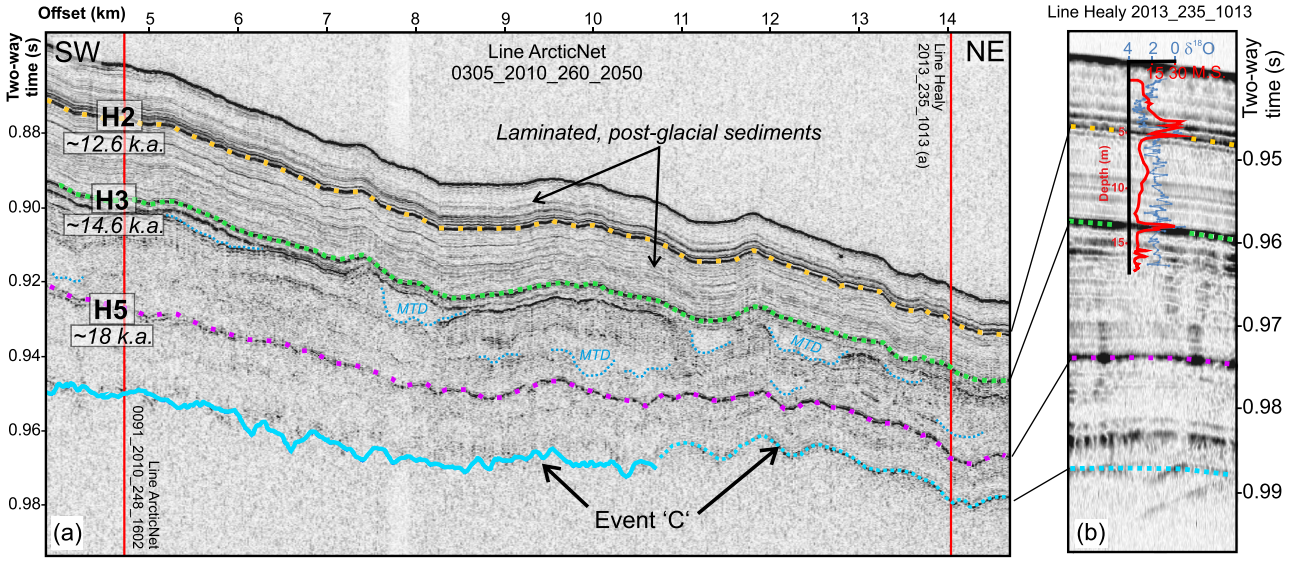

FIGURE 9 (a) Example of 3.5 kHz sub-bottom profiler data (ArcticNet line 0305_2010_260_2050) across Pokak (location see Figure 3) showing uppermost 60–70 m of layered sediments. The grooved surface of 'event C' (blue solid line is surface from three-dimensional data, dotted line is continuation of horizon in 3.5 kHz data) is overlain by up to 10 m laminated sediments conformably filling the grooved surface. This laminated sequence is capped by reflection event (H5) above which abundant mass transport deposits (MTDs) are present (dotted cyan lines). Above this interval of MTDs, sediments are uniformly stratified. (b) Correlation of core-derived magnetic susceptibility (MS, red) and $\delta^{18}O$ isotope data (blue) from the Healy 2013 expedition to sub-bottom data with ages of horizons based on radiocarbon dates (Keigwin et al., 2018; Klotsko et al., 2019). See Supporting Information Figures S7 and S8 for regional correlation of all these horizons [Color figure can be viewed at wileyonlinelibrary.com]

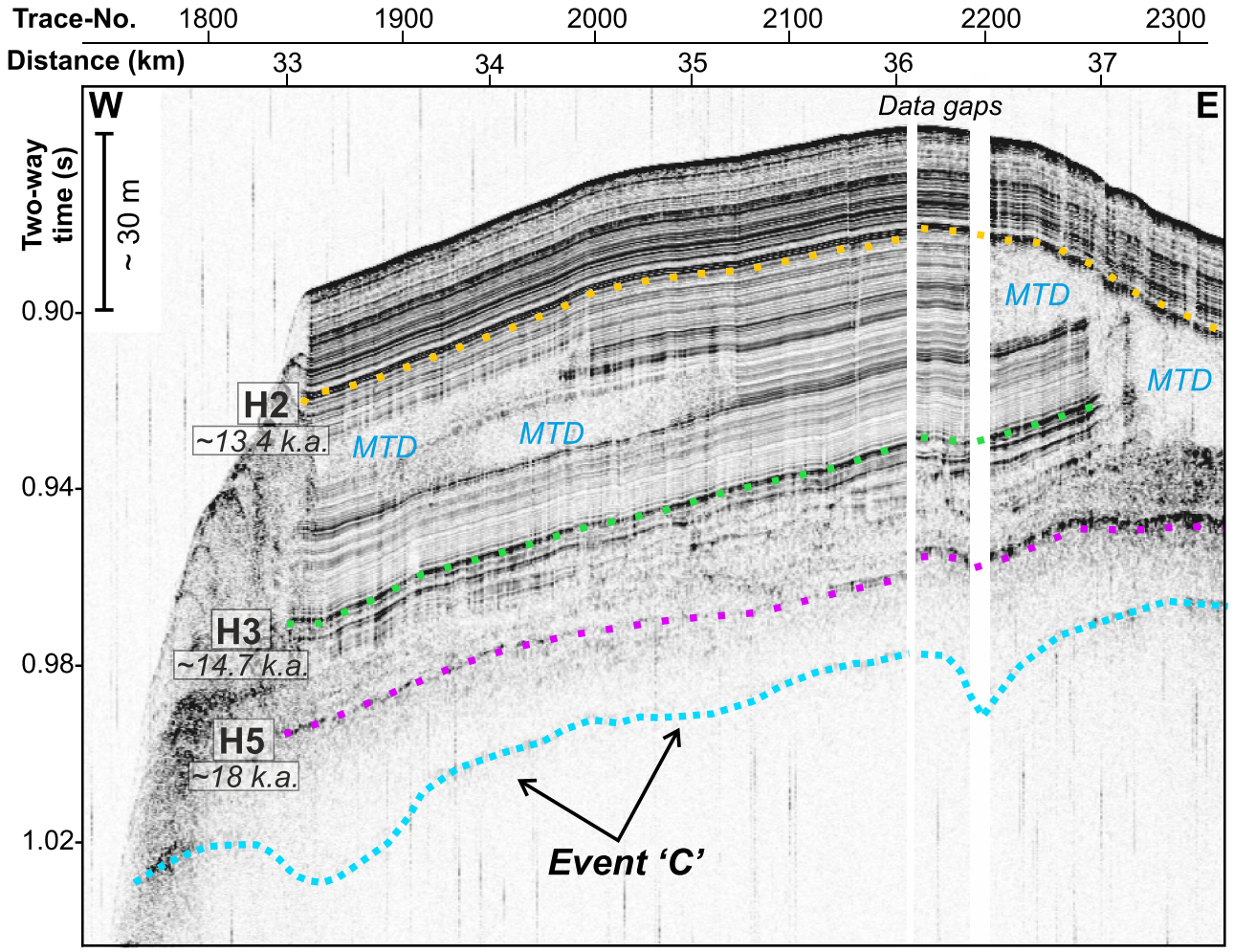

FIGURE 10 Example of 3.5 kHz sub-bottom profiler data across Ajurak (location see Figure 3) showing uppermost 60–70 m of sediment. The grooved surface of 'event C' is seen overlain by a cover of laminated sediments, conformably filling the grooved surface. The reflection of 'event B' is not imaged here and below the limit of penetration of the sounder system. Approximate ages (extrapolated below H3) were assigned to horizons based on available radiocarbon dates and high-resolution sub-bottom profiler data across the region (compare to Figure 9; Blasco et al., 2013; Cameron & King, 2019; Keigwin et al., 2018; King et al., 2017; Klotsko et al., 2019; Saint-Ange et al., 2014) [Color figure can be viewed at wileyonlinelibrary.com]

character of the lineations. Clearly, 'event A' is significantly older than events B and C.

6.3 | Regional implications

Our analyses of the buried MSGL features on the continental slope suggest movement of a grounded ice mass across our study area from the northeast to southwest, parallel to the slope contours. This direction is not consistent with a glacial ice source from the Mackenzie Trough to the west or from the mainland immediately to the south (Figure 1). The most likely source is from the Canadian Arctic Archipelago to the east. The question becomes whether our lineated surfaces resulted from a clockwise-rotating extensive ice shelf which was grounded in a narrow band where its Beaufort Sea margin impacted the upper slope (analogous to the process described by Jakobsson et al. [2016]), or whether the ice streams emanating from continental shelf troughs remained fully grounded as they followed the upper slope contours.

In this regard, lineations similar in morphology to our slope-situated examples have been described across the Canadian Arctic Archipelago on land (Dyke, 2008; Hodgson, 1994; Stokes et al., 2005, 2006; Vincent, 1983, 1990; Vincent et al., 1984) and on the continental shelf in both Amundsen Gulf (Batchelor et al., 2013b, 2014; MacLean et al., 2015) and M'Clure Strait (Batchelor et al., 2016; Batchelor & Dowdeswell, 2014). These are attributed to ice streaming from sources in the Arctic Islands westward out of glacially excavated troughs onto the continental shelf (Batchelor et al., 2013b, 2014, 2016; MacLean et al., 2010, 2015). Whereas the glacial sediment succession in the inner shelf areas is very thin, further offshore on the shelf, Batchelor et al. (2014) and Stokes et al. (2006) have described thick deposits of glacial sediments that they refer to as the M'Clure and Amundsen trough mouth fans. It is unclear from these studies what the ice thickness was. However, eight sequences making up the Amundsen fan are interpreted as stacked till sheets with the base of the succession being marked by an erosional unconformity that is up to 700 m below the seafloor (Batchelor et al., 2014). In this context, ice emanating from the troughs appears to be thinner than the grounding depth required to form the youngest two lineated horizons (presumably of LGM age). This, in combination with the groove-like nature of the lineations (i.e., an erosional character) suggest that the lineations we observe may not be formed by continuously grounded

ice streams but are rather associated with an ice shelf that locally grounded.

The orientation of our lineations suggesting ice movement to the southwest is also puzzling. Irrespective of the grounding depths, ice emanating freely from M'Clure Strait would be expected to trend in a west-northwest direction while ice from Amundsen Gulf would likely trend to the northwest (see Figure 1). This raises a question of what conditions could in theory so strongly deflect movement of a grounded ice mass from the trough axes to a slope parallel orientation. Full assessment of this topic will require further research; however, a buttressing (confining) force could be a reasonable mechanism to both thicken and deflect the ice stream or its floating (shelf) component. Given the different flow directions and possible volumes of ice emanating from M'Clure Strait *versus* Amundsen Gulf, it is also possible that complex interactions occurred between the grounded and floating ice masses. These interactions may have deflected flow direction and or formed a melange with ice build up from two sources. There are also possibilities of course that large-scale oceanic processes such as the Beaufort Gyre may have affected movement of the floating ice mass, also impacting the ice shelf. Our study also suggests a possible lift-off depth between grounded and floating ice at ~800 m present day water depth and an upper contact limit at ~220 m. This range in water depths indicates that the base of the ice shelf was not entirely horizontal.

As summarized on Figure 1, several authors have attributed glacial lineations similar to those that we describe to possible western flow along the Beaufort margin (Engels et al., 2008) and the Chukchi Borderlands (Jakobsson et al., 2005, 2008, 2010, 2016; Polyak et al., 2001). Our observations are consistent with this interpretation, providing further evidence that during glacial times an extensive ice shelf occupied the Arctic Ocean and grounded along the upper slope over a distance exceeding 1000 km. On their own, our findings do not dictate complete Arctic ice shelf cover. However, they fill in an important regional gap confirming a source of ice for such a hypothetical ice shelf in the Canadian Arctic Archipelago. This adds to a body of evidence consistent with and corroborating a rotating (clockwise) ice shelf acting as an integral mass, interacting with the entire Beaufort Sea margin and possibly, as suggested by earlier studies, the entire Arctic Basin.

Jakobsson et al. (2010) studied glaciogenic features from the Lomonosov Ridge north of Greenland, Morris Jesup Rise, and Yermak Plateau and concluded that an extensive ice shelf may have existed in the Arctic Ocean during MIS 6 (*c.* 130 ka) associated with the penultimate glaciation. Given the burial depths of the even 'A' horizon, it is possible that these lineations formed during a Mid-Pleistocene glaciation and could therefore be associated with the ice shelf during MIS 6 proposed by Jakobsson et al. (2010). The regionally much better preserved MSGL of events B and C are younger than MIS 6 and associated with the last glacial period based on our acoustic stratigraphy and ^{14}C dating. Thus, a similar ice shelf as proposed by Jakobsson et al. (2010) for MIS 6 may also have existed during the LGM that locally grounded along the southern Beaufort Sea margin. Vast offshore ice could have provided a buttress to the ice that flowed from the Canadian Arctic Archipelago and drove the overall westward drift of the ice shelf. Whether an ice shelf covered much of the Arctic Ocean during the LGM (MIS 2), similarly to as proposed by Jakobsson et al. (2016) for the penultimate glaciation (MIS 6), or grounded locally along the Beaufort Sea margin cannot be addressed with the data at hand.

The depth difference between events B and C is relatively small and the sediment record between those two horizons is barely imaged with our data set. However, seismic data show that the intervening sediment unit, where present, has an acoustically transparent to weakly laminated character (Figures 3b and 6). The ice shelf that produced the lineations on surface 'B' is therefore suggested to have lifted off and/or retreated to shallower grounding depths during this interval, enabling some postglacial sediments to be deposited, before it re-grounded to form the shallowest set of lineations on surface 'C'.

7 | CONCLUSIONS

Using 3D and 2D seismic survey data from the outer continental shelf and upper continental slope in the southern Canadian Beaufort Sea we have mapped and characterized three buried unconformities with large-scale, parallel grooves that are interpreted as mega-scale glacial lineations formed from grounding of an ice shelf. The lineations occur along the upper slope in water depths between 220 and 800 m and are oriented in a northeast–southwest direction. The two shallowest events ('B' and 'C') are closely spaced, have similar orientations and spatial extent suggesting that they may be similar in age, but formed during different grounding events. They have a thin and discontinuous cover of sediments that is acoustically transparent to poorly stratified, and are conformably overlain by 40–80 m of well stratified sediments. Using high resolution 2D acoustic sub-bottom profiler and published age data we have considered the age of the two youngest MSGL events by examining the sediment cover on top of the surface. Correlations with dated horizons in a 17 m long stratigraphic core suggest that these two lineated surfaces were formed sometime prior to 18 ka and may be related to the LGM. The deepest MSGL of 'event A' is much older and may have been formed during the penultimate glaciation (MIS 6).

Grooves from the shallowest two MSGL-horizons become broader and less frequent to the southwest, indicating ice movement in this direction. All of the lineations follow the continental shelf break and slope contours with their orientation suggesting a source of the ice from the Canadian Arctic Archipelago with possible coalesced flow from Amundsen Gulf and M'Clure Strait. The MSGLs are interpreted to have been formed by the grounding of an ice shelf that was fed, in part, by ice streams emanating from Amundsen Gulf and M'Clure Strait. Observations of similar grooved surfaces along the slope offshore of northern Alaska and further to the west suggest the possibility of a vast interconnected ice shelf in the Arctic Ocean that may have extended more than 1000 km from its source in the Canadian Arctic Archipelago during the penultimate glaciation (MIS 6). Our observations of three lineated surfaces of different sub-seabed depth suggests that such ice shelves may have developed several times during the Quaternary with varied grounding histories.

ACKNOWLEDGEMENTS

The authors would like to thank Imperial Oil Resources Canada Ltd and British Petroleum Canada for kindly providing access to the 3D seismic data volumes Ajurak and Pokak for geohazard analyses. Additional thanks go to Michelle Côté and Roger McLeod from the

Geological Survey of Canada-Pacific for general support in generating maps and figures. This research was supported by project number 20160247 funded by the Ministry of Oceans and Fisheries, Korea. This is Natural Resource Canada contribution number 2020-0421.

CONFLICT OF INTEREST

The authors declare that they have no known competing financial interests or personal relationships that could have appeared to influence the work reported in this article.

DATA AVAILABILITY STATEMENT

Data (seafloor bathymetry and sub-bottom profiler) from the ArcticNet programme are available online through the main web page of the University of New Brunswick, Arctic Mapping Programme: http://www.omg.unb.ca/arctic-mapping/. The 3D seismic data volumes were provided by Imperial Oil Resources Canada Ltd and British Petroleum Canada to Natural Resources Canada, but remain confidential. Additional data can be requested from scientists at the Geological Survey of Canada (curator Michelle Côté, michelle.cote@canada.ca) or through the Open Government Portal available online at: https://open.canada.ca/data/en/dataset?organization=nrcan-rncan&q=geoscience.

ORCID


Michael Riedel https://orcid.org/0000-0001-5729-4482

REFERENCES

Barendregt, R.W., Vincent, J.S., Irving, E. & Baker, J. (1998) Magnetostratigraphy of quaternary and late tertiary sediments on Banks Island, Canadian Arctic Archipelago. *Canadian Journal of Earth Sciences*, 35(2), 147–161. https://doi.org/10.1139/e97-094

Batchelor, C.L. & Dowdeswell, J.A. (2014) The physiography of High Arctic cross-shelf troughs. *Quaternary Science Reviews*, 92, 68–96. https://doi.org/10.1016/j.quascirev.2013.05.025

Batchelor, C.L., Dowdeswell, J.A., Dowdeswell, E. & Toff, B.J. (2016) A subglacial landform assemblage on the outer shelf of M'Clure Strait, Canadian Arctic, ploughed by iceberg keels, Atlas of Submarine Glacial Landforms: Modern, Quaternary and Ancient; by Dowdeswell, J A (ed.); Canals, M (ed.); Jakobsson, M (ed.); Todd, B J (ed.); Dowdeswell, E K (ed.); Hogan, K A (ed.). *Geological Society, Memoirs*, 46(1), 337–340. https://doi.org/10.1144/M46.143

Batchelor, C.L., Dowdeswell, J.A. & Pietras, J.T. (2013a) Seismic stratigraphy, sedimentary architecture and palaeo-glaciology of the Mackenzie Trough: Evidence for two Quaternary ice advances and limited fan development on the western Canadian Beaufort Sea margin. *Quaternary Science Reviews*, 65, 73–87. https://doi.org/10.1016/j.quascirev.2013.01.021

Batchelor, C.L., Dowdeswell, J.A. & Pietras, J.T. (2013b) Variable history of Quaternary ice-sheet advance across the Beaufort Sea margin, Arctic Ocean. *Geology*, 41(2), 131–134. https://doi.org/10.1130/g33669.1

Batchelor, C.L., Dowdeswell, J.A. & Pietras, J.T. (2014) Evidence for multiple Quaternary ice advances and fan development from the Amundsen Gulf cross-shelf trough and slope, Canadian Beaufort Sea margin. *Marine and Petroleum Geology*, 52, 125–143. https://doi.org/10.1016/j.marpetgeo.2013.11.005

Batchelor, C.L., Margold, M., Krapp, M., Murton, D.K., Dalton, A.S., Gibbard, P.L. *et al.* (2019) The configuration of Northern Hemisphere ice sheets through the Quaternary. *Nature Communications*, 10(1), 3713. https://doi.org/10.1038/s41467-019-11601-2

Bellwald, B., Planke, S., Lebedeva-Ivanova, N., Piasecka, E.D. & Andreassen, K. (2019) High-resolution landform assemblage along a buried glacio-erosive surface in the SW Barents Sea revealed by P-Cable 3D seismic data. *Geomorphology*, 332, 33–50. https://doi.org/10.1016/j.geomorph.2019.01.019

Bellwald, B., Planke, S., Piasecka, E.D., Matar, M.A. & Andreassen, K. (2018) Ice-stream dynamics of the SW Barents Sea revealed by high-resolution 3D seismic imaging of glacial deposits in the Hoop area. *Marine Geology*, 402, 165–183. https://doi.org/10.1016/j.margeo.2018.03.002

Blasco, S., Bennett, R., Brent, T., Burton, M., Campbell, P., Carr, E. *et al.* (2013) 2010 state of knowledge: Beaufort Sea seabed geohazards associated with offshore hydrocarbon development. Geological Survey of Canada Open File 6989: 340. https://doi.org/10.4095/292616

Blasco, S.M., Fortin, G., Hill, P.R., O'Connor, M.J. & Brigham-Grette, J. (1990) The late Neogene and Quaternary stratigraphy of the Canadian Beaufort continental shelf. *The Geology of North America*, 50, 491–502. https://doi.org/10.1130/DNAG-GNA-L.491

Boulton, G.S. & Clark, C.D. (1990) A highly mobile Laurentide ice sheet revealed by satellite images of glacial lineations. *Nature*, 346(6287), 813–817. https://doi.org/10.1038/346813a0

Cameron, G.D.M. & King, E.L. (2019) Mass-failure complexes on the central Beaufort Slope, offshore Northwest Territories. Geological Survey of Canada Open File 8356: 39. https://doi.org/10.4095/314644

Canals, M., Urgeles, R. & Calafat, A.M. (2000) Deep sea-floor evidence of past ice streams off the Antarctic Peninsula. *Geology*, 28(1), 31–34. https://doi.org/10.1130/0091-7613(2000)028<0031:DSEOPI>2.0.CO;2

Carter, L.D., Brouwers, E.M. & Marincovich, M., Jr. (1988) Nearshore marine environments of the Alaskan Beaufort Sea during deposition of the Flaxman Member of the Gubik Formation, in: JP Galloway, TD Hamilton (Eds.), Geologic studies in Alaska by the US Geological Survey during 1987. *US Geological Survey Circular*, 1016 (1988), 27–30.

Clark, C.D. (1993) Mega-scale glacial lineations and cross-cutting ice-flow landforms. *Earth Surface Processes and Landforms*, 18(1), 1–19. https://doi.org/10.1002/esp.3290180102

Clark, C.D., Tulaczyk, S.M., Stokes, C.R. & Canals, M. (2003) A groove-ploughing theory for the production of mega-scale glacial lineations, and implications for ice-stream mechanics. *Journal of Glaciology*, 49(165), 240–256. https://doi.org/10.3189/172756503781830719

Cofaigh, C.Ó., Dowdeswell, J.A., Allen, C.S., Hiemstra, J., Pudsey, C.J., Evans, J. & Evans, D.J. (2005) Flow dynamics and till genesis associated with a marine-based Antarctic palaeo-ice stream. *Quaternary Science Reviews*, 24(5–6), 709–740. https://doi.org/10.1016/j.quascirev.2004.10.006

Cofaigh, C.Ó., Livingstone, S.J. & Dowdeswell, J.A. (2016) Mega-scale glacial lineations in Marguerite Trough, Antarctic Peninsula. *Geological Society, London, Memoirs*, 46(1), 175–176. https://doi.org/10.1144/M46.72

Dalton, A., Atkinson, N., Batterson, M., Carlson, A., Tarasov, L., Larson, P. *et al.* (2020) An updated radiocarbon-based ice margin chronology for the last deglaciation of the North American Ice Sheet Complex. *Quaternary Science Reviews*, 234, 106223. https://doi.org/10.1016/j.quascirev.2020.106223

Denton, G.H. & Hughes, T.J. (1983) Milankovitch theory of ice ages: Hypothesis of ice-sheet linkage between regional insolation and global climate. *Quaternary Research*, 20(2), 125–144. https://doi.org/10.1016/0033-5894(83)90073-X

Dietrich, J.R., Chen, Z., Chi, G., Dixon, J., Hu, K. & McNeil, D. (2010) Petroleum plays in Upper Cenozoic Strata in the Beaufort–Mackenzie Basin, Arctic Canada. American Association of Petroleum Geologists, Annual Meeting Abstracts, 1 p., available online at (accessed 26 March 2020). http://www.searchanddiscovery.com/pdfz/documents/2011/10300dietrich/ndx_dietrich.pdf.html

Dietrich, J.R., Coflin, K.C., Lane, L.S., Dixon, J. & Cook, F.A. (1989) Interpretation of deep seismic reflection data, Beaufort Sea, Arctic Canada. Geological Survey of Canada, Open File 2106, 15. https://doi.org/10.4095/130756

Dietrich, J.R., Dixon, J. & McNeil, D. (1985) Sequence analysis and nomenclature of Upper Cretaceous to Holocene strata in the Beaufort–Mackenzie basin. Geological Survey of Canada, Paper no. 85-1A, 613–628. https://doi.org/10.4095/130756.

Dixon, J. (1996) Geological atlas of the Beaufort–Mackenzie area. *Geological Survey of Canada, Miscellaneous Report*, 59, 173. https://doi.org/10.4095/207658s

Dixon, J. & Dietrich, J.R. (1990) Canadian Beaufort Sea and adjacent land areas. In: Grantz, A., Johnson, L. & Sweeney, J.F. (Eds.) *The Arctic Ocean Region: The Geology of North America*. Boulder, Colorado: Geological Society of America, pp. 239–256. https://doi.org/10.1130/DNAG-GNA-L

Dixon, J., Dietrich, J.R. & McNeil, D. (1992) Upper Cretaceous to Pleistocene sequence stratigraphy of the Beaufort–Mackenzie and Banks Island areas, northwest Canada. Geological Survey of Canada, Bulletin 407, 90. https://doi.org/10.4095/133237

Dowdeswell, J.A., Jakobsson, M., Hogan, K.A., O'Regan, M., Backmanb, J., Evans, J. *et al*. (2010) High-resolution geophysical observations of the Yermak Plateau and northern Svalbard margin: Implications for ice-sheet grounding and deep-keeled icebergs. *Quaternary Science Reviews*, 29(25-26), 3518–3531. https://doi.org/10.1016/j.quascirev.2010.06.002

Dowdeswell, J.A., Ottesen, D. & Rise, L. (2016) 3D seismic imagery of mega-scale glacial lineations and flow-switching by ice streams on the Norwegian continental shelf. *Geological Society, London, Memoirs*, 46(1), 181–182. https://doi.org/10.1144/M46.96

Dowdeswell, J.A., Ottesen, D., Rise, L. & Craig, J. (2007) Identification and preservation of landforms diagnostic of past ice-sheet activity on continental shelves from three-dimensional seismic evidence. *Geology*, 35(4), 359–362. https://doi.org/10.1130/G23200A.1

Duk-Rodkin, A. & Hughes, O.L. (1994) Tertiary-Quaternary drainage of the pre-glacial Mackenzie basin. *Quaternary International*, 22, 221–241. https://doi.org/10.1016/1040-6182(94)90015-9

Dyke, A.S. (2004) An outline of North American deglaciation with emphasis on central and northern Canada. In: Ehlers, J., Gibbard, P.L. (Eds.). *Developments in Quaternary Sciences*, 2(B), 373–424. https://doi.org/10.1016/S1571-0866(04)80209-4

Dyke, A.S. (2008) The Steensby Inlet Ice Stream in the context of the deglaciation of Northern Baffin Island, Eastern Arctic Canada. *Earth Surface Processes and Landforms*, 33(4), 573–592. https://doi.org/10.1002/esp.1664

Dyke, A.S., Andrews, J.T., Clark, P.U., England, J.H., Miller, G.H., Shaw, J. & Veillette, J.J. (2002) The Laurentide and Innuitian ice sheets during the Last Glacial Maximum. *Quaternary Science Reviews*, 21(1-3), 9–31. https://doi.org/10.1016/S0277-3791(01)00095-6

Dyke, A.S., Moore, A. & Robertson, L. (2003) Deglaciation of North America: Thirtytwo digital maps at 1:7,000,000 scale with accompanying digital chronological database and one poster (two sheets) with full map series. Geological Survey of Canada Open File 1574. https://doi.org/10.4095/214399

Ely, J.C., Clark, C.D., Spagnolo, M., Stokes, C.R., Greenwood, S.L., Hughes, A.L. *et al*. (2016) Do subglacial bedforms comprise a size and shape continuum? *Geomorphology*, 257, 108–119. https://doi.org/10.1016/j.geomorph.2016.01.001

Engels, J.L., Edwards, M.H., Polyak, L. & Johnson, P.D. (2008) Seafloor evidence for ice shelf flow across the Alaska Beaufort margin of the Arctic Ocean. *Earth Surface Processes and Landforms*, 33(7), 1047–1063. https://doi.org/10.1002/esp.1601

England, J., Atkinson, N., Bednarski, J., Dyke, A.S., Hodgson, D.A. & Ó Cofaigh, C. (2006) The Innuitian Ice Sheet: Configuration, dynamics and chronology. *Quaternary Science Reviews*, 25(7–8), 689–703. https://doi.org/10.1016/j.quascirev.2005.08.007

Flood, R.D. (1983) Classification of sedimentary furrows and a model for furrow initiation and evolution. *Geological Society of America Bulletin*, 94(5), 630–639. https://doi.org/10.1130/0016-7606(1983)94<630:COSFAA>2.0.CO;2

Fowler, A.C. (2000) An instability mechanism for drumlin formation. In: Maltman, A., Hambrey, M.J. & Hubbard, B. (Eds.) *Deformation of Glacial Materials*, Special Publication of the Geological Society, The Geological Society London, Vol. 176. Bath, UK: The Geological Society Publishing House, pp. 307–319. https://doi.org/10.1144/GSL.SP.2000.176.01.23

Fowler, A.C. (2009) Instability modelling of drumlin formation incorporating leeside cavity growth. *Proceedings of the Royal Society of London, Series A*, 466(2109), 2673–2694. https://doi.org/10.1098/rspa.2008.0490

Grosswald, M.G. & Hughes, T.J. (2008) The case for an ice shelf in the Pleistocene Arctic Ocean. *Polar Geography*, 31(1–2), 69–98. https://doi.org/10.1080/10889370802175929

Hindmarsh, R.C.A. (1998) The stability of a viscous till sheet coupled with ice flow, considered at wavelengths less than the ice thickness. *Journal of Glaciology*, 44(147), 285–292. https://doi.org/10.3189/S0022143000002628

Hodgson, D.A. (1994) Episodic ice streams and ice shelves during retreat of the northwesternmost sector of the Wisconsinan Laurentide Ice Sheet over the central Canadian Arctic archipelago. *Boreas*, 23, 14–28.

Jakobsson, M., Andreassen, K., Bjarnadóttir, L.R., Dove, D., Dowdeswell, J.A., England, J.H. *et al*. (2014) Arctic Ocean glacial history. *Quaternary Science Reviews*, 92, 40–67. https://doi.org/10.1016/j.quascirev.2013.07.033

Jakobsson, M., Gardner, J.V., Vogt, P.R., Mayer, L.A., Armstrong, A., Backman, J. *et al*. (2005) Multibeam bathymetric and sediment profiler evidence for ice grounding on the Chukchi Borderland, Arctic Ocean. *Quaternary Research*, 63(2), 150–160. https://doi.org/10.1016/j.yqres.2004.12.004

Jakobsson, M., Mayer, L.A., Coakley, B., Dowdeswell, J.A., Forbes, S., Fridman, B. *et al*. (2012) The International Bathymetric Chart of the Arctic Ocean (IBCAO) Version 3.0. *Geophysical Research Letters*, 39(12), L12609. https://doi.org/10.1029/2012GL052219

Jakobsson, M., Nilsson, J., Anderson, L., Backman, J., Björk, G., Cronin, T.M. *et al*. (2016) Evidence for an ice shelf covering the central Arctic Ocean during the penultimate glaciation. *Nature Communications*, 7(1), 10365. https://doi.org/10.1038/ncomms10365

Jakobsson, M., Nilsson, J., O'Regan, M., Backman, J., Löwemark, L., Dowdeswell, J.A. *et al*. (2010) An Arctic Ocean ice shelf during MIS 6 constrained by new geophysical and geological data. *Quaternary Science Reviews*, 29(25–26), 3505–3517. https://doi.org/10.1016/j.quascirev.2010.03.015

Jakobsson, M., Polyak, L., Edwards, M., Kleman, J. & Cakley, B. (2008) Glacial geomorphology of the Central Arctic Ocean: the Chukchi Borderland and the Lomonosov Ridge. *Earth Surface Processes and Landforms*, 33(4), 526–545. https://doi.org/10.1002/esp.1667

Jin, Y.J. & Dallimore, S.R. (2016) ARA05C Marine Research Expedition – Canada–Korea–USA Beaufort Sea Geoscience Research Program: Summary of 2014 Activities. Geological Survey of Canada, Open File Report 7999, 107. https://doi.org/10.4095/297866

Jin, Y.K., Riedel, M., Hong, J.K., Nam, S.I., Jung, J.Y., Ha, S.Y. *et al*. (2015) Overview of field operations during a 2013 research expedition to the southern Beaufort Sea on the RV Araon. Geological Survey of Canada, Open File 7754, 180. https://doi.org/10.4095/295856

Johnson, R.G. & Andrews, J.T. (1986) Glacial terminations in the oxygen isotope record of deep sea cores: hypothesis of massive Antarctic ice-shelf destruction. *Palaeogeography, Palaeoclimatology, Palaeoecology*, 53(2–4), 107–138. https://doi.org/10.1016/0031-0182(86)90041-6

Keigwin, L.D., Klotsko, S., Zhao, N., Reilly, B., Giosan, L. & Driscoll, N.W. (2018) Deglacial floods in the Beaufort Sea preceded Younger Dryas cooling. *Nature Geoscience*, 11(8), 599–604. https://doi.org/10.1038/s41561-018-0169-6

King, E.C., Hindmarsh, R.C.A. & Stokes, C.R. (2009) Formation of mega-scale glacial lineations observed beneath a West Antarctic ice stream. *Nature Geoscience*, 2(8), 585–588. https://doi.org/10.1038/ngeo581

King, E.L., Li, M., Wu, Y., Forest, A., Blasco, S., Harrison, P. *et al*. (2017) A belt of seabed erosion along the Beaufort Sea margin, offshore

Northwest Territories, governed by Holocene evolution of the Beaufort Shelf-break Jet; geological evidence, current measurements, and initial oceanographic modelling; Geological Survey of Canada, Open File 8198, 1 poster. https://doi.org/10.4095/299691

Klotsko, S., Driscoll, N. & Keigwin, L. (2019) Multiple meltwater discharge and ice rafting events recorded in the deglacial sediments along the Beaufort Margin, Arctic Ocean. *Quaternary Science Reviews*, 203, 185–208. https://doi.org/10.1016/j.quascirev.2018.11.014

Livingstone, S.J., Stokes, C.R., Cofaigh, C.Ó., Hillenbrand, C.-D., Vieli, A., Jamieson, S.S. *et al.* (2016) Subglacial processes on an Antarctic ice stream bed. 1: Sediment transport and bedform genesis inferred from marine geophysical data. *Journal of Glaciology*, 62(232), 270–284. https://doi.org/10.1017/jog.2016.18

MacCarthy, G.R. (1958) Glacial boulders on the Arctic coast of Alaska, Arctic, 11, 70-85, available online at: http://pubs.aina.ucalgary.ca/Arctic/Arctic11-2-70.pdf (accessed 7 September 2020).

MacLean, B., Blasco, S., Bennett, R., England, J., Rainey, W., Hughes-Clarke, J. & Beaudoin, J. (2010) Ice keel seabed features in marine channels of the Canadian Arctic Archipelago: evidence for former ice streams and iceberg scouring. *Quaternary Science Reviews*, 29(17-18), 2280–2301. https://doi.org/10.1016/j.quascirev.2010.05.032

MacLean, B., Blasco, S., Bennett, R., Hughes-Clarke, J. & Patton, E. (2016) Crag-and-tail features, Amundsen Gulf, Canadian Arctic Archipelago. *Geological Society, London, Memoirs*, 46(53–54), 2016–2054. https://doi.org/10.1144/M46.84

MacLean, B., Blasco, S., Bennett, R., Lakeman, T., Hughes-Clarke, J., Kuus, P. & Patton, E. (2015) New marine evidence for a Late Wisconsinan ice stream in Amundsen Gulf, Arctic Canada. *Quaternary Science Reviews*, 114, 149–165. https://doi.org/10.1016/j.quascirev.2015.02.003

McNeil, D., Duk-Rodkin, A., Dixon, J., Dietrich, J.R., White, J., Miller, K. & Issler, D. (2001) Sequence stratigraphy, biotic change, 87Sr/86SR record, paleoclimatic history, and sedimentation rate change across a regional late Cenozoic unconformity in Arctic Canada. *Canadian Journal of Earth Science*, 38(2), 309–331. https://doi.org/10.1139/e00-098

Mercer, J.H. (1970) A former ice sheet in the Arctic Ocean? Palaeogeography, Palaeoclimatology. *Palaeoecology*, 8(1), 19–27. https://doi.org/10.1016/0031-0182(70)90076-3

Niessen, F., Hong, J.-K., Hegewald, A., Mathiessen, J., Stein, R., Kim, H. *et al.* (2013) Repeated Pleistocene glaciation of the East Siberian continental margin. *Nature Geoscience*, 6(10), 842–846. https://doi.org/10.1038/ngeo1904

Niessen, F., Matthiessen, J. & Stein, R. (2010) Sedimentary environment and glacial history of the Northwest Passage (Canadian Arctic Archipelago) reconstructed from high-resolution acoustic data. *Polarforschung*, 79(2), 65–80.available online at https://epic.awi.de/id/eprint/22476/1/Nie2010b.pdf (accessed 7 September 2020).

Polyak, L., Edwards, M.H., Coakley, B.J. & Jakobsson, M. (2001) Ice shelves in the Pleistocene Arctic Ocean inferred from glaciogenic deep-sea bedforms. *Nature*, 410(6827), 453–457. https://doi.org/10.1038/35068536

Rafaelsen, B., Andreassen, K., Kuilman, L.W., Lebesbye, E., Hogstad, K. & Midtbo, M. (2002) Geomorphology of buried glacigenic horizons in the Barents Sea from three-dimensional seismic data. In glacier-influenced sedimentation on high-latitude continental margins, (eds.) Dowdeswell JA, Ó Cofaigh C. *Geological Society of London, Special Publication*, 203(1), 259–276. https://doi.org/10.1144/GSL.SP.2002.203.01.10

Rampton, V.N. (1982) Quaternary geology of the Yukon Coastal Plain. *Geological Survey of Canada Bulletin*, 317, 49 (4 sheets). https://doi.org/10.4095/111347

Rampton, V.N. (1988) Quaternary Geology of the Tuktoyaktuk Coastlands. Northwest Territories, Geological Survey of Canada. Memoir 423, 98. https://doi.org/10.4095/126937

Riedel, M., Hong, J.K., Jin, Y.K. & Rohr, K.M.M. (2016) Structural interpretation and velocity analyses of multichannel seismic data acquired with the icebreaker ARAON across the southern Beaufort Seja for regional hazard implications – first results. *Geological Survey of Canada, Current Research*, 2016–3, 24. https://doi.org/10.4095/298840

Rohr, K.M.M., Riedel, M., Dallimore, S.R. & Côté, M.M. (2021) Slope fan and glacial sedimentation on the central Beaufort continental slope, Arctic Canada. *Geological Survey of Canada, Current Research*, 2021, 18. https://doi.org/10.4095/326068

Saint-Ange, F., Kuus, P., Blasco, S., Piper, D.J.W., Clarke, J.H. & MacKillop, K. (2014) Multiple failure styles related to shallow gas and fluid venting, upper slope Canadian Beaufort Sea, northern Canada. *Marine Geology*, 355, 136–149. https://doi.org/10.1016/j.margeo.2014.05.014

Scambos, T.A., Bohlander, J.A., Shuman, C.A. & Skvarca, P. (2004) Glacier acceleration and thinning after ice shelf collapse in the Larsen B embayment, Antarctica. *Geophysical Research Letters*, 31(18), L18402. https://doi.org/10.1029/2004GL020670

Shaw, J., Pugin, A. & Young, R.R. (2008) A meltwater origin for Antarctic shelf bedforms with special attention to megalineations. *Geomorphology*, 102(3–4), 364–375. https://doi.org/10.1016/j.geomorph.2008.04.005

Spagnolo, M., Bartholomaus, T.C., Clark, C.D., Stokes, C.R., Atkinson, N., Dowdeswell, J.A. *et al.* (2017) The periodic topography of ice stream beds: Insights from the Fourier spectra of mega-scale glacial lineations. *Journal of Geophysical Research – Earth Surface*, 122(7), 1355–1373. https://doi.org/10.1002/2016JF004154

Spagnolo, M., Clark, C.D., Ely, J.C., Stokes, C.R., Anderson, J.B., Andreassen, K. *et al.* (2014) Size, shape and spatial arrangement of mega-scale glacial lineations from a large and diverse dataset. *Earth Surface Processes and Landforms*, 39, 1432–1448. https://doi.org/10.1002/esp.3532

Stokes, C.R., Clark, C.D., Darby, D.A. & Hodgson, D.A. (2005) Late Pleistocene ice export events into the Arctic Ocean from the M'Clure Strait Ice Stream, Canadian Arctic Archipelago. *Global and Planetary Change*, 49(3–4), 139–162. https://doi.org/10.1016/j.gloplacha.2005.06.001

Stokes, C.R., Clark, C.D. & Windsborrow, M.C.M. (2006) Subglacial bedform evidence for a major palaeo-ice stream and its retreat phases in Amundsen Gulf. *Canadian Arctic Archipelago, Journal of Quaternary Science*, 21(4), 399–412. https://doi.org/10.1002/jqs.991

Tasianas, A., Bünz, S., Vadakkepuliyambatta, S. & Mienert, J. (2016) Buried subglacial landforms in the SW Barents Sea imaged using high-resolution P-Cable seismic data. *Geological Society, London, Memoirs*, 46(1), 183–184. https://doi.org/10.1144/M46.117

Tulaczyk, S.M., Scherer, R.P. & Clark, C.D. (2001) A ploughing model for the origin of weak tills beneath ice streams: A qualitative treatment. *Quaternary International*, 86(1), 59–70. https://doi.org/10.1016/S1040-6182(01)00050-7

Vaughan, J.M., England, J.H. & Evans, D.J. (2014) Glaciotectonic deformation and reinterpretation of the Worth Point stratigraphic sequence: Banks Island, NT, Canada. *Quaternary Science Reviews*, 91, 124–145. https://doi.org/10.1016/j.quascirev.2013.11.005

Vincent, J.S. (1983) La géologie du Quaternaire et la géomorphologie de l'Ile Banks, arctique Canadien. Geological Survey of Canada, Memoir 405, 118.

Vincent, J.S. (1990) Late Tertiary and Early Pleistocene deposits and history of Banks Island, southwestern Canadian Arctic Archipelago. *Arctic*, 43(4) Late Tertiary Arctic Environments and Biostratigraphy, 339–363.

Vincent, J.S., Morris, W.A. & Occhietti, S. (1984) Glacial and non-glacial sediments of Matuyama paleomagnetic age on Banks Island. *Canadian Arctic Archipelago Geology*, 12, 139–142.

Woodworth-Lynas, C., Blasco, S., Duff, D., Fowler, J., Iṣler, E.B., Landva, J. *et al.* (2016a) Geophysical and geological data compilation outer shelf and upper slope, Southern Beaufort Sea: A handbook of geohazard conditions, Section 1. Environmental Studies Research Fund Publication 208-1, 36 pp. with Appendices. https://www.esrfunds.org/sites/www.esrfunds.org/files/publications/ESRF208-1-Woodworth-Lynas-Blasco.pdf

Woodworth-Lynas, C., Blasco, S., Duff, D., Fowler, J., Işler, E.B., Landva, J. *et al*. (2016b) Geophysical and geological data compilation outer shelf and upper slope, Southern Beaufort Sea: A handbook of geo-hazard conditions, Section 2. Environmental Studies Research Fund Publication 208-2, 181 pp. with Appendices and nine Enclosures. https://www.esrfunds.org/sites/www.esrfunds.org/files/publications/ESRF208-2-Woodworth-Lynas-Blasco.pdf and https://www.esrfunds.org/sites/www.esrfunds.org/files/publications/ESRF208-2-Enclosures_Woodworth-Lynas,%20Blasco.pdf

Woodworth-Lynas, C.M.T., Simms, A. & Rendell, C.M. (1985) Iceberg grounding and scouring on the Labrador Continental Shelf. *Cold Regions Science and Technology*, 10(2), 163–186. https://doi.org/10.1016/0165-232X(85)90028-X

SUPPORTING INFORMATION

Additional supporting information may be found online in the Supporting Information section at the end of this article.

How to cite this article: Riedel M, Dallimore S, Wamsteeker M, et al. Mega-scale glacial lineations formed by ice shelf grounding in the Canadian Beaufort Sea during multiple glaciations. *Earth Surf. Process. Landforms*. 2021;46:1568–1585. https://doi.org/10.1002/esp.5125